Pharmacological analysis of ionotropic glutamate and GABA receptor function in neuronal circuits of the zebrafish olfactory bulb

Inaugural – Dissertation

zur Erlangung der Doktorwürde

der Naturwissenschaftlich-Mathematischen Gesamtfakultät

der Ruprecht-Karls-Universität Heidelberg

Vorgelegt 2008 in Heidelberg von

Diplom Biologe Rico Tabor

geboren in Weisswasser

Die vorliegende Arbeit wurde in der Abteilung Biomedizinische Optik am Max-Planck-Institut für medizinische Forschung in Heidelberg durchgeführt unter der Leitung von PD Dr. Rainer W. Friedrich.

Wesentliche Teile dieser Arbeit wurden vorab veröffentlicht:
Tabor, R. & Friedrich R.W. (2008). Pharmacological analysis of ionotropic glutamate receptor function in neuronal circuits of the zebrafish olfactory bulb. PloS ONE 3(1):e1416

Gutachter:

Prof. Dr. Stephan Frings	Universität Heidelberg
Prof. Dr. Winfried Denk	Max-Plank-Institut für medizinische Forschung in Heidelberg

Hiermit erkläre ich, dass ich die vorliegende Arbeit selbstständig unter Anleitung verfasst und keine anderen als die angegebenen Quellen als Hilfsmittel benutzt habe.

---	---
Datum	Unterschrift

Abstract

In the olfactory bulb and other brain areas, basic cellular and synaptic properties of individual neurons have been studied extensively in reduced preparations. Nevertheless, it is still poorly understood how intactions among multiple neurons shape spatio-temporal activity patterns and give rise to the computational properties of the the intact circuit.

In this thesis, I used pharmacological manipulations of excitatory and inhibitory neurotransmitter receptors to examine the synaptic interactions underlying spontaneous and odor-evoked activity patterns in the intact OB of zebrafish. Electrophysiological and conventional and two-photon calcium imaging methods were used to record activity from the principal neurons of the OB (mitral cells), their sensory input, and local interneurons.

The combined blockade of AMPA/kainate and NMDA receptors abolished odor-evoked excitation of mitral cells (MCs), indicating that sensory input to the OB is mediated by ionotropic glutamate receptors. Surprisingly, however, the blockade of AMPA/Kainiate receptors alone increased the mean response of MCs and decreased the mean response of interneurons (INs). The blockade of NMDA receptors alone caused little or no change in the mean responses of MCs and INs. In addition, antagonists of both glutamate receptor types had diverse effects on the magnitude and time course of individual MC and IN responses and, thus, changed spatio-temporal activity patterns across neuronal populations. The blockade of GABA(A) receptors increased spontaneous and odor evoked firing rates of mitral cells and often induced rhythmic bursting. Moreover, the blockade of, GABA(A) or AMPA/kainate receptors abolished fast oscillatory activity in the local field potential. Blockade of GABA(B) receptors reduced calcium influx into terminals of afferent sensory axons and modulated response time courses of mitral cells.

These results indicate that (1) IN activity during an odor response depends mainly on AMPA/Kainiate receptor input, (2) interactions between MCs and INs regulate the total OB output activity, (3) AMPA/Kainiate receptors and GABA(A) receptors underly the synchronization of odor-dependent neuronal ensembles and (4) odor-specific patterns of OB output activity are shaped by circuits containing iGlu receptors and GABA receptors. These results provide insights into the mechanisms underlying the processing of odor-encoding activity patterns in the OB.

Zusammenfassung

Im olfaktorischen Bulbus (OB) und anderen Hirnarealen wurden grundlegende zelluläre und synaptische Eigenschaften der Einzelneurone ausführlich in reduzierten Präparaten studiert. Trotzdem ist kaum bekannt, wie die Interaktionen mehrerer Nervenzellen untereinander räumlich-zeitlich strukturierte Aktivitätsmuster formen und dadurch die rechnerischen Eigenschaften der intakten Schaltkreise entstehen.

In dieser Arbeit nutzte ich pharmakologische Manipulationen der erregenden und hemmenden Neurotransmitter-Rezeptoren, um die synaptischen Interaktionen zu untersuchen, die spontanen und geruchsinduzierten Aktivitätsmustern im intakten OB des Zebrafisch zugrunde liegen. Methoden der Elektrophysiology sowie der konventionellen und Zwei-Photonen-Mikroskopie wurden genutzt, um Aktivität von Ausgangsneuronen des OB (Mitralzellen, MCs), ihrem sensorischen Eingang, und Interneuronen (INs) zu messen.

Die gleichzeitige Blockierung von AMPA/Kainate- und NMDA-Rezeptoren verhinderte die geruchsinduzierte Erregung von MCs, was darauf hinweist, dass der sensorische Eingang des OB durch ionotrope Glutamatrezeptoren vermittelt wird. Die Blockierung von AMPA/Kainate Rezeptoren allein jedoch erhöhte überraschender Weise im Mittel die Antwort von MCs und reduzierte im Mittel die Antwort von INs. Die Blockierung von NMDA Rezeptoren allein lösten im Mittel geringe oder keine Veränderung der Antworten von MCs and INs aus. Außerdem hatten die Antagonisten für beide Glutamatrezeptoren unterschiedliche Einflüsse auf Größe und Zeitverlauf individueller MC- und IN- Antworten und veränderten daher das räumlich-zeitliche Aktivitätsmuster innerhalb der Nervenzellpopulation. Die Blockierung von GABA(A)-Rezeptoren erhöhte spontane und geruchsinduzierte Feuerraten in MCs und induzierten oft rhythmische, stoßweise Aktivität. Die Blockierung von GABA(A)- und AMPA/Kainate-Rezeptoren hob überdies geruchsinduzierte Oszillationen im Feldpotenzial auf. Die Blockierung von GABA(B)-Rezeptoren verringerte den Kalziumeinstrom in die Endigungen afferenter sensorischer Axone und modulierte den Zeitverlauf von MC-Antworten.

Die Ergebnisse zeigen, dass (1) die Aktivität der Interneurone während der Geruchsantwort hauptsächlich von AMPA/Kainate-Rezeptoren abhängt, (2) die Interaktionen zwischen Mitralzellen und Interneuronen die Gesamtaktivität des Ausgangssingnales des olfaktorischen Bulbus regulieren, (3) AMPA/Kainate-Rezeptoren und GABA(A)-Rezeptoren der Synchronisation geruchsabhängiger Gruppen von Nervenzellen zugrunde liegen und (4) geruchsspezifische Muster im Ausgangssignal des olfaktorischen Bulbus durch Schaltkreise

geformt werden, die iGlu Rezeptoren und GABA Rezeptoren enthalten. Diese Ergebnisse ermöglichen Einblick in die Mechanismen die der Verarbeitung geruchskodierender Aktivitätsmuster im olfaktorischen Bulbus unterliegen.

Table of contents

Abbreviations 3
Introduction 5
The structure of the olfactory bulb 6
Functional properties of the vertebrate olfactory bulb 9
Ionotropic glutamate receptors 10
GABA receptors 11
Role of ionotropic glutamate and GABA receptors for odor processing 13
Role of reciprocal synapses in network activity 13
GABA release in the reciprocal synapse 14
GABA(B) receptors mediated presynaptic inhibition of sensory input 15
Objective of this thesis 16
Materials and Methods 17
Animals, preparation and odor stimulation 17
Pharmacological agents 17
Electrophysiological recordings 18
Calcium Imaging 19
Two-photon Ca^{2+}-imaging 19
Conventional Ca^{2+}-imaging with a camera 21
Data analysis 21
Results 23
Pharmacological investigation of GABA receptor function in the olfactory bulb 23
Presynaptic inhibition of olfactory sensory neuron terminals by GABA(B) receptors 23
Effect of GABA(B) receptor blockade on mitral cell odor responses 25
Effect of GABA(A) receptor blockade on mitral cell odor responses 28
Effect of GABA(A) receptor blockade on odor evoked oscillations in the local field potential 33
Pharmacological investigations of ionotropic glutamate receptor function in the olfactory bulb 34
Combined blockade of AMPA receptors and NMDA receptors 34
Blockade of AMPA receptors: effect on mitral cell responses 36
Blockade of NMDA receptors: effects on mitral cell responses 39
Effects of ionotropic glutamate receptor antagonists on local field potential oscillations 42
Measurements of odor-evoked activity patterns by two-photon Ca^{2+}-imaging 43
Effects of ionotropic glutamate receptor antagonists on interneuron activity 46
Discussion 49
Functions of presynaptic inhibition of sensory input by GABA(B) receptors 49
Receptors involved in the regulation of neuronal excitability 52
AMPA receptor-dependent control of interneuron activity and mitral cell inhibition 56
GABA(A) and AMPA receptors are required for odor-evoked rhythmical synchronization 57
Slow temporal modulations of MC response patterns 58
Functional implications and outlook 59
Acknowledgements 61
References 62

Abbreviations

AMPA	alpha-amino-3-hydroxy-5-methyl-isoxazole proprionic acid
AP5	D-(-)-2-Amino-5-phosphonopentanoic acid, specific antagonist for NMDA receptors
Ca^{2+}	calcium
CGP54626	CGP54626 hydrochloride, chemical name: [S-(R*,R*)]-[3-[[1-(3,4-Dichlorophenyl)ethyl]amino]-2-hydroxypropyl](cyclohexylmethyl) phosphinic acid, specific antagonist for GABA(B) receptors
Cl^-	chloride
GABA	gamma-aminobutyric acid
HCO_3^-	hydrogen carbonate
iGlu receptor	ionotropic glutamate receptor
IN	interneuron
K^+	potassium
LFP	local field potential
MC	mitral cell
Mg^{2+}	magnesium
Na^+	sodium
NBQX	2,3-Dioxo-6-nitro-1,2,3,4-tetrahydrobenzo[f]quinoxaline-7-sulfonamide, antagonist for AMPA receptors
NMDA	N-methyl-D-aspartate
OB	olfactory bulb
OSN	olfactory sensory neuron
PSTH	peri-stimulus time histogram

Introduction

Olfaction is an evolutionarily old and essential sense for vertebrates. Important behaviors such as the search for food and mating partners or the detection of predators and harmful substances are guided by olfaction. Odor processing in the olfactory system needs to provide reliable information on identity and category of usually complex odors, as well as on changes in the olfactory environment and concentration gradients. The first olfactory processing center in vertebrates is the OB. Tissue and cell structure, synaptic connectivity, transmitter substances, and properties of biophysical membranes and response characteristic of neuron types have been investigated in reduced systems such as brain slices. Other experiments were done in the intact brain to study odor-evoked activity and functional properties of the system. However, it is still unclear how properties of the system arise from the interactions of individual neurons in the circuit. This bridge between investigations at the cellular and systems level is necessary to understand the mechanistic basis of neuronal circuit function.

Here I studied functions of the OB network during the processing of odor-evoked activity patterns in the intact brain. The major excitatory and inhibitory pathways in the system were chosen for pharmacological manipulations. Effects were analysed with respect to synaptic circuitries and some hypothesis on odor processing mechanisms provided from structural and functional studies.

The major excitatory transmitter in the OB is glutamate. The most important receptors are the ionotropic glutamate receptors of the types NMDA and AMPA/Kainate. The main inhibitory transmitter is GABA with the receptors of the types GABA(A) and GABA(B). An explant of the whole brain from zebrafish (*Danio rerio*) with attached nose was chosen as model system for several reasons. The zebrafish OB is anatomically and functionally similar to those of higher vertebrates but much smaller. This has two major advantages. First, explanted functional brains can easily be maintained for hours in standardized solutions. Measurments are bare of artefacts from heartbeat and breathing but can be performed with natural odor stimulation of the nose and provide approaches for intracellular recordings. Second, optical methods benefit from good light penetration and allow for the simultaneous observation of large numbers of individual neurons by two-photon Ca^{2+} imaging. Amino acids are known to be natural odor stimuli for fish and were used in addition to extracts from commercial fish food. The zebrafish was established as model system for the study of spatio-

temporal activity patterns in the intact OB. A substantial amount of data exists from previous studies of odor processing in this system.

The structure of the olfactory bulb

Odors are transduced into neuronal activity by OSNs located in the olfactory epithelium inside the nose. Each of those cells is thought to express only one olfactory receptor out of a large repertoire of genes (Vassar et al., 1993; Ressler et al., 1994); but also see (Goldman et al., 2005). There are 143 different olfactory receptor genes in the zebrafish (Alioto and Ngai, 2005) and even more than 1400 genes in mice (Zhang et al., 2004). OSN project unbranched axons to the surface of the (OB).

Functional and morphological properties of the OB are highly conserved across all vertebrates (Allison, 1953; Andres, 1970) and even share many features with the corresponding structure in insects, the antennal lobe. Several layers can be distinguished in the OB (Satou, 1990; Shepherd et al., 2004). Common to mammals and fish are olfactory nerve layer, glomerular layer, MC layer and internal cell layer. In mammals in addition the inner and the outer plexiform layer are distuingished, which enclose the MC layer. The outer layer of the OB is the olfactory nerve layer which contains axons from OSNs. These axons ramify in distinct neuropil modules called glomeruli. Axons from OSNs expressing the same receptor molecule converge and terminate in the same glomerulus konvergieren (Ressler et al., 1994; Vassar et al., 1994; Mombaerts et al., 1996). OSNs release the excitatory neurotransmitter glutamate onto the output neurons of the OB, the MCs, and a subset of INs, the juxtaglomerular cells. Juxtaglomerular cells are a heterogeneous group of cells mediating predominantly inhibitory effects on MCs. Periglomerular cells are the major subgroup of these neurons and possess mainly short processes. Dendrites extensively ramify inside glomeruli and provide GABAergic synaptic input to MCs, the same or other periglomerular cells and inhibit transmitter release from the axon terminals of OSNs by paracrine activation of GABA(B) receptors (Smith and Jahr, 2002; Murphy et al., 2005). In mammals a subgroup of juxtaglomerular cells with longer axons, called short axon cells, appears to excite remote periglomerular cells and exerts long range inhibition of MCs (Aungst et al., 2003). MCs are glutamatergic and project axons to multiple higher brain centres. They interact with INs in the glomerular layer and INs in the inner plexiform layer which are called granule cells. INs are

activated through dendrodendritic synapses and axon collaterals and feed back inhibition through reciprocal or unidirectional synapses via GABA release (Fig. 1).

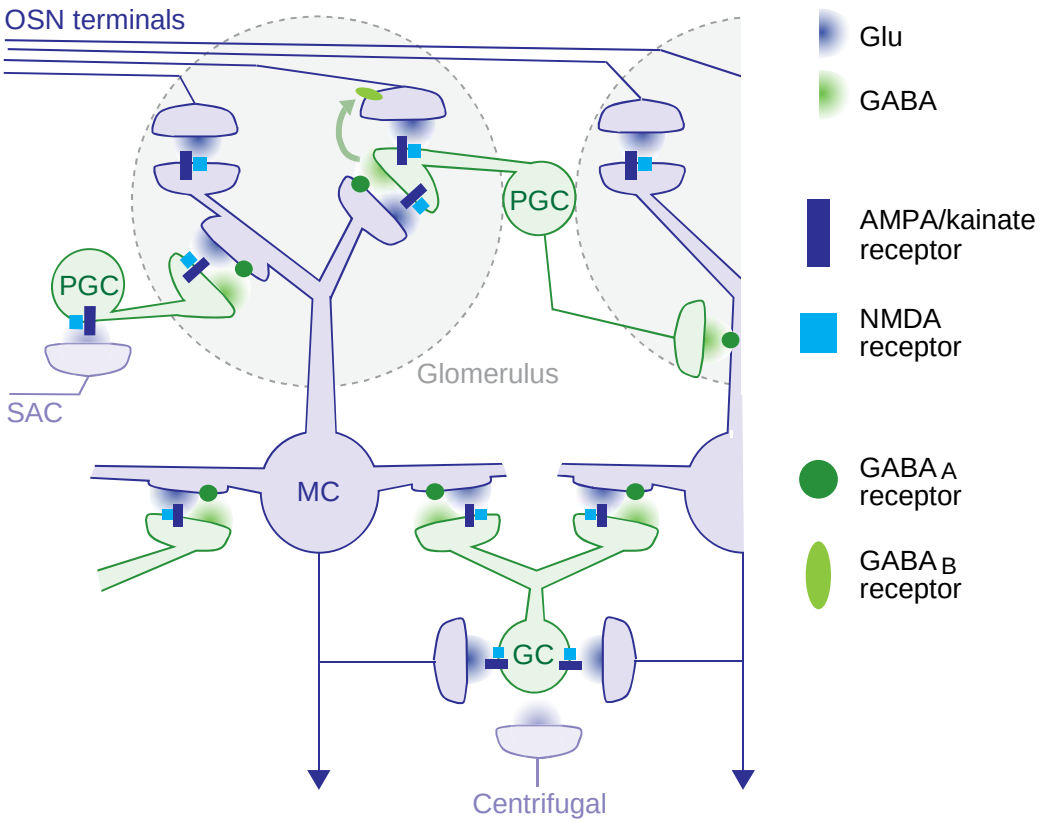

Figure 1. Simplified architecture of synaptic pathways in the OB. Within glomeruli, glutamatergic OSNs provide excitatory synaptic input to MCs and a subpopulation of periglomerular cells via AMPA receptors and NMDA receptors. Periglomerular cells also receive glutamatergic input from MC dendrites and provide GABAergic output to MCs of the same and neighbouring glomeruli. In addition, GABA (green arrow) and dopamine (not shown) released from periglomerular cells reduces glutamate release from OSN axon terminals by acting on GABA(B) and D_2 receptors, respectively, in the same glomerulus (Nickell et al., 1994; Hsia et al., 1999; Wachowiak and Cohen, 1999a; Aroniadou-Anderjaska et al., 2000; Murphy et al., 2005; Wachowiak et al., 2005a). In subglomerular layers, glutamate release from MC dendrites and axon collaterals stimulates axonless granule cells via AMPA receptors and NMDA receptors. Granule cells release GABA back onto $GABA_A$ receptors on the same and other MCs. Glutamate release from a MC can therefore cause recurrent inhibition of the same MC and lateral inhibition of other MCs via periglomerular and granule cells. These interactions, here collectively referred to as the MC→IN→MC pathway, can extend over distances corresponding to multiple glomeruli. An additional pathway mediating lateral inhibition that is not detailed in this scheme is the short axon cell →periglomerular→MC pathway identified in rodents (Aungst et al., 2003; Wachowiak and Shipley, 2006). Centrifugal inputs from higher brain areas are also not shown in detail. Many of these inputs terminate on INs and are glutamatergic. Not included in the scheme are metabotropic glutamate receptors, interactions between INs in the granule cell layer (Pressler and Strowbridge, 2006), glutamate spillover (Isaacson, 1999a), and a small glutamatergic subpopulation of granule cells (Didier et al., 2001). Abbreviations: OSN: olfactory sensory neuron, PGC: periglomerular cell, MC: mitral cell, GC: granule cell, SAC: short axon cell.

The main receptors for glutamate are the ionotropic NMDA and AMPA receptors which are co-localized at the OSN→MC synapse and at MC→IN synapses (Sassoe-Pognetto and Ottersen, 2000; Shepherd et al., 2004). Released GABA inhibits MC activity and OSN axon terminals via GABA(A) and GABA(B) receptors. Within glomeruli, MCs can excite each other via gap junctions and fast volume transmission of glutamate (Aroniadou-Anderjaska et al., 1999a; Schoppa and Westbrook, 2002; Urban and Sakmann, 2002; Christie et al., 2005). Across glomeruli, synaptic interactions are mediated by INs, predominantly periglomerular and granule cells (Shepherd et al., 2004; Wachowiak and Shipley, 2006, Fig. 1). The most prominent inter-glomerular synaptic pathway is the MC→IN→MC pathway, where periglomerular or granule cells are excited by glutamatergic MC→IN synapses and feed back GABAergic inhibition onto the same and other MCs at IN→MC synapses.

The olfactory network receives centrifugal input from multiple higher brain areas. Retrograde labeling studies in rodents revealed input from the anterior olfactory nucleus, locus coeruleus, raphe nuclei, ventral hippocampal rudiment, dorsal peduncular cortex, piriform cortex, lateral olfactory tract, medial septal area, diagonal band of Broca and the hypothalamus (Broadwell and Jacobowitz, 1976; Macrides et al., 1981). Cortical fibers were found to excite granule cells by activation of NMDA and AMPA receptors (Pinching and Powell, 1972; Luskin and Price, 1983; Laaris et al., 2007) Input from basal forebrain structures, the diagonal band of Broca and the substantia innominata, are partially cholinergic and partially GABAergic (Mesulam et al., 1983; Ichikawa and Hirata, 1986; Zaborszky et al., 1986) and project throughout all layers of the OB (Carson and Burd, 1980; Macrides et al., 1981; Ichikawa and Hirata, 1986; Gomez et al., 2006) Acetylcholine modulates activity of INs and MCs through activation of nicotinic and muscarinic receptors (Castillo et al., 1999; Pressler et al., 2007) and is involved in olfactory learning (Wilson et al., 2004). The role of GABAergic fibers is, to my knowledge, not investigated. Fibers from raphe nuclei are serotoninergic (McLean and Shipley, 1987) and innervate all layers of the OB but with particular high density inside glomeruli. Serotonin depolarizes MCs and INs (Tani et al., 1992; Hardy et al., 2005) and appears to be involved in olfactory learning (McLean et al., 1996) and odor discrimination (Moriizumi et al., 1994). The locus coeruleus is the origin of noradrenergic projections (Fallon and Moore, 1978; Shipley et al., 1985). Noradrenalin can reduce spontaneous activity in GCs and MCs (Czesnik et al., 2001) but also directly excite MCs (Hayar et al., 2001).

In fish the major centrifugal input arises from the telencephalon and terminates presumably on granule cells (Satou, 1990). Centrifugal fibers apparently play a role for odor

learning (Kiselycznyk et al., 2006), which was also suggested for the zebrafish (Satou et al., 2006) and influence network oscillations (Martin et al., 2006).

Functional properties of the vertebrate olfactory bulb

Each OSN detects a spectrum of different molecules while each molecule can activate several different types of OSNs ((Sicard and Holley, 1984; Shepherd, 1994; Buck, 1996; Dulac, 1997; Friedrich and Korsching, 1997; Duchamp-Viret et al., 1999; Malnic et al., 1999). The response profiles of individual glomerli are therefore broad and overlapping and the information provided by the response of a single glomerulus is limited. Glomeruli are thought to be independent units because OSN axons in one glomerulus respond very similarly to odor stimulation (Wachowiak et al., 2004) and associated MCs show correlated activity (Buonviso and Chaput, 1990; Carlson et al., 2000; Schoppa and Westbrook, 2002; Urban and Sakmann, 2002). Therefore, odors are encoded in a combinatorial fashion by patterns of activity across the array of glomeruli ((Leveteau and MacLeod, 1966; Stewart et al., 1979; Shepherd, 1994; Dulac, 1997; Friedrich and Korsching, 1997; Mori et al., 1999; Wachowiak and Cohen, 2001), Glomeruli with similar response profiles tend to build clusters (Friedrich and Korsching, 1998; Wachowiak and Cohen, 2001; Mori et al., 2006). Different odor classes as amino acids, bile acids or nucleotides evoke responses in specific regions of the zebrafish OB which only partially overlap (Friedrich and Korsching, 1998). Chemically closely related substances as amino acids with long side chain, basic side chain or aromatic side chain activate glomeruli in segregated subregions (Friedrich and Korsching, 1997). In mice segregated groups of glomeruli show different preferences for functional groups of substances with similar carbon chains (Wachowiak and Cohen, 2001) and aliphatic aldehydes of increasing carbon chain length evoked systematically shifting responses along a rostral-caudal strip of the dorsal bulb (Belluscio and Katz, 2001). The hierarchically mapping of chemical properties across the array of glomeruli is referred to as chemotopy.

In contrast to OSNs, odor responses of MCs do not follow a stereotyped phasic-tonic time course (Meredith, 1986; Hamilton and Kauer, 1989; Wellis et al., 1989; Buonviso et al., 1992; Friedrich and Laurent, 2001; Luo and Katz, 2001; Tabor et al., 2004). The firing frequency is dynamically changed in an odor- and cell-specific manner. Particularly during the first few hundreds of milliseconds after stimulus onset firing rates can change rapidly. Phases of excitation can be followed by inhibition or vice versa. In the zebrafish, odor-evoked activity patterns are reorganized over time, leading to reduced overlap between

representations of related odors (Friedrich and Laurent, 2001; Friedrich et al., 2004; Friedrich and Laurent, 2004). This pattern decorrelation might be useful for fine discriminations of similar odors and for other computations in higher brain areas.

Odor-evoked responses in the OB are further temporally structured by fast oscillations, which were measured by field potential recordings in many species (Adrian, 1942; Bressler and Freeman, 1980; Gray and Skinner, 1988; Gelperin and Tank, 1990; Laurent and Davidowitz, 1994; Lam et al., 2000; Friedrich et al., 2004) These oscillations likely reflect rhythmical interactions between MCs and INs. It was shown that subpopulations of MCs can become synchronized in odor-dependent ensembles (Kashiwadani et al., 1999; Laurent, 2002; Friedrich et al., 2004). In the zebrafish the separate analysis of synchronized and non-synchronized action potentials revealed that activity patterns made up of synchronized action potentials remain similar over time for related odors, whereas activity patterns made up of non-synchronized action potentials undergo decorrelation. The high correlation of synchronized action potential patterns in response to related odors might preserve information on odor similarity. The parrallel transmission of odor category by synchronous spikes and odor identity by asynchronous activity might be an example for multiplexing in brain activity (Friedrich et al., 2004). Temporal modulations of MC firing during an odor response and rhythmical synchronizations of OB neurons change odor representations and temporally structure odor evoked activity. Feedback from inhibitory INs inside the network is likely to play an important role for these dynamics.

Ionotropic glutamate receptors

Glutamate is recognized by special receptor proteins in the membrane of neurons that either are ionotropic glutamate (iGlu) receptors, which are ligand-gated ion channels or metabotropic glutamate receptors, which are G-protein coupled receptors. The family of iGlu receptors has been separated according to specific agonists into NMDA, AMPA and Kainate receptors. Receptor properties were extensively discussed elsewhere (Dingledine et al., 1999). Briefly, functional iGlu receptors are assemblies of four subunits (Rosenmund et al., 1998; Tichelaar et al., 2004). All subunits have a common basic structure. The long N-terminal is located in the extracellular space. Adjacent to the transmembrane domain (TM-I) it contains a sequence (S1) that is one of two domains responsible for transmitter binding. The second sequence (S2) is part of an extracellular loop between the third and fourth transmembrane

domain (TM-III and TM-IV). The second transmembrane domain (TM-II) does not cross the membrane, but returns to the intracellular site. In the protein complex TM-II domains form the ion-channel. The intracellular C-terminal, following TM-IV, interacts with the cytosceleton and signal proteins and is target for modulations at several phosphorylation sites. A substantial number of subunit isoforms arise from splice variation of this region.

In physiological studies AMPA and Kainate receptors have traditionally been lumped together as "non-NMDA-receptors". The historically late development of specific antagonists against Kainate receptors hampered the scientific progress in this field. The traditional separation is nowadays often kept as the functionally well described NMDA receptor is, in contrast to the other two iGlu receptors, in addition voltage dependent.

NMDA receptors are inactive at resting membrane potentials. In physiological concentration of Mg^{2+} a depolarization is required before the ion pore can be activated by transmitter binding. NMDA receptor subunits are NR1, four types of NR2 (NR2A-D) and NR3. Most functional neuronal receptors are composed of two NR1 subunits and two NR2 subunits. In addition to glutamate also glycine is needed to activate this receptor. Glycine is bound by the NR1 subunits and glutamate is bound at the junction of NR1 and NR2. Upon opening the channel allows Na^{+}-, K^{+}- and Ca^{2+}-ions to cross the membrane leading to depolarization. The high permeability for Ca^{2+}-ions is thought to be crucial for the induction of synaptic plasticity (Miyamoto, 2006). In the experiments reported here, NMDA receptors were blocked by AP5, which is a widely used specific antagonist.

AMPA receptors mediate fast glutamatergic cation-currents leading to transient depolarization of postsynaptic membrane (Jonas, 2000). Subunits are GluR1-4. Most neuronal AMPA receptors contain GluR2 subunits (Isaac et al., 2007) and are Ca^{2+}-impermeable. The subunit composition is often specific to the type of neuron and plays a role for synaptic plasticity (Derkach et al., 2007; Liu and Zukin, 2007; Shepherd and Huganir, 2007). Here I used NBQX to pharmacologically interfere with these receptors. NBQX blocks AMPA receptors with high affinity but also blocks Kainate receptors (Sheardown et al., 1990).

GABA receptors

GABAergic synaptic transmission is found throughout the whole brain (Sivilotti and Nistri, 1991). There are three types of GABA receptors. GABA(B) receptors are metabotropic receptors. Pharmacological properties were used to divide ionotropic GABA receptors into

GABA(A) and GABA(C) receptors but this separation is still controversial (Barnard et al., 1998; Bormann, 2000)

The predominant type of GABA receptors is the GABA(A) receptor. The relevance of this receptors for clinical treatment of anxiety, epilepsy and sleep disorders led to intense investigations and detailed clarification of molecular structure and physiological function (for review see: Nutt, 2006; Michels and Moss, 2007). Briefly, upon GABA binding an ion-channel is opened, which is permeable for Cl^--ions and to some extend to HCO_3^-. The effect is a stabilization of the resting potential and inhibition of neuronal activity by hyperpolarization or shunting. Synaptic currents are usually phasic while extrasynaptic receptors can mediate tonic inhibition. GABA(A) receptors belong to the superfamily of nicotinic ligand-gated ion channels. Other members of this family are nicotinic acetylcholine receptors, glycin receptors and the $5HT_3$ serotonine receptors. Functional GABA(A) receptors are composed of five subunits arranged as a ring around the central pore. Receptors are functionally heterogeneous caused by a large number of subunits. Subunits are grouped into α with isoforms 1-6, β with isoforms 1-4, γ with isoforms 1-3, δ, ε and σ subunits. The number of isoforms can vary from species to species. The most common GABA(A) receptor consists of two α1, two β2 and one γ2 subunits but the subunit composition is often specific to the type of neuron and even to the subcompartmental localization of the receptor. The binding site for GABA is located between α and β subunits. Each subunit consists of four transmembrane domains (TM1-TM4). The large N-terminus and the short C-terminus are directed to the extracellular space. A large loop between TM3 and TM4 carries domains for intracellular interactions. TM2 provides the lining of the ion pore.

Clinically most relevant GABA(A) modulators are Benzodiazepines. They bind to a modulatory site distinct from the GABA binding site. An allosteric change leads to increased efficiency of the receptor without direct activation. In the work described here GABA(A) receptors were blocked by gabazine, which has no clinical relevance. Gabazine is specific for GABA(A) receptors and competes with GABA for the GABA binding site (Ueno et al., 1997).

GABA(B) receptors act through activation of a G-protein. The receptor has diverse synaptic functions (for review see: Calver et al., 2002; Kornau, 2006). Presynaptic receptors suppress transmitter release by inhibition of voltage gated Ca^{2+}-channels or second messenger effects on vesicle priming. Postsynaptic receptors usually hyperpolarize neurons by activation of K^+-channels. They are also involved in synaptic plasticity. In addition GABA(B) receptors are often extrasynaptically expressed. Activation of these receptors is thought to depend on

transmitter spill-over from distant release sites (Isaacson, 2000). Increases in extrasynaptic transmitter concentrations are unlikely to arise from weak activity. These receptors therefore might respond to synchronous activity or hyperexcitation.

Only two types of GABA(B) receptors subunits were found. They belong to family C of the superfamily of 7-transmembrane G protein-coupled receptors as also metabotropic glutamate receptors do. The GABA(B1) subunit exists in two isoforms, GABA(B1a) and GABA(B1b), which both combine with GABA(B2) subunits to heteromeric dimers forming the functional receptor. The intracellular C-terminus forms a coiled-coil structure involved in heterodimerization. The N-terminal contains a venus flytrap module responsible for transmitter binding. GABA(B1) is sufficient for transmitter binding but dimerisation increases the affinity and is needed for G protein coupling. In this work these receptors were blocked by CGP54626, which is a specific antagonist with high affinity. In some Ca^{2+}-imaging experiments the specific agonist Baclofen was used to activate GABA(B) receptors.

Role of ionotropic glutamate and GABA receptors for odor processing

Role of reciprocal synapses in network activity

Important synaptic contacts in the OB are reciprocal dendrodendritic synapses between MCs and INs, where both cell types are pre- and postsynaptic at the same time. Glutamate mediated excitation of INs can evoke GABA release locally in the same synapse that released the glutamate. If the excitatory signal spreads throughout the dendritic tree, GABA release is also evoked from other, remote synapses. These synaptic connections can produce recurrent feedback inhibition onto activated MCs (Jahr and Nicoll, 1982; Isaacson and Strowbridge, 1998) and laterally inhibit neighboring MCs (Yokoi et al., 1995; Isaacson and Strowbridge, 1998). The impact of recurrent and lateral inhibition during odor processing in the intact olfactory system, however, is not clear.

Reciprocal synapses are likely to be involved in the generation of rhythmic neuronal activity. The release of glutamate from activated MCs elicits release of GABA from INs. This suppresses MC activity and leads to a decay of the excitatory signal in INs. The reduced release of GABA then allows MCs to recover from inhibition and become active again. The fast GABA(A) receptors which mediate the inhibition of MCs appear to be crucial for the generation of rhythmical neuronal activity in the OB (Lagier et al., 2004; Schoppa, 2006a). As

both, MCs and INs, are synaptically connected to multiple partners the rhythmic activity can synchronize action potential firing in many cells.

The lateral coupling of MCs through inhibitory INs might also be involved in other network properties as sharpening of odor response profiles (Yokoi et al., 1995; Uchida et al., 2000) or slow temporal modulations of firing patterns leading to decorrelation of initially similar representations of different odors (Friedrich and Laurent, 2004). Furthermore, inhibitory feedback might be crucial for the regulation of network excitability and total output strength. The amplitude and complexity of sensory input varies considerably dependent on the odor stimulus (Friedrich and Laurent, 2004). To keep firing frequencies of the neurons in an appropriate range some sort of gain control mechanism must exist. GABA(A) receptors appear likely candidates as their blockade leads to hyperexcitability and epileptiform activity in the brain (McCormick and Contreras, 2001).

To understand the relative contribution of reciprocal synaptic interactions to the different mechanisms it might help to clarify how the GABA release from INs is evoked during odor processing. If INs preferentially release GABA locally restricted at the sites of direct glutamatergic excitation rhythmic synchronization of activated MCs might be the dominant function, while global dendritic GABA release suggested an important role for functions dependent on lateral inhibition, as sharpening of odor response profiles or slow temporal patterning.

GABA release in the reciprocal synapse

Brief electrical stimulations of MCs are typically followed by longlasting inhibitory signals in MCs. It was obsered that those long-lasting events are composed from discrete synaptic events with rapid decay time courses (Wellis and Kauer, 1993; Schoppa et al., 1998) The underlying synaptic pathway is assumed to be the MC→IN→MC pathway. The glutamate released form MCs activates NMDA and AMPA receptors which are colocated in dendritic synapses of INs (Sassoe-Pognetto and Ottersen, 2000; Shepherd et al., 2004). This evokes release of GABA from INs leading to activation of GABA(A) receptors in MC membranes. The prolonged period of inhibition in MCs following brief pulse stimulations therefore appears to come from an asynchronous GABA release from INs.

In the hippocampus it was hypothezised that asynchrounous transmitter release depends on prolonged presynaptic Ca^{2+}-signals (Hefft and Jonas, 2005). Such prolonged Ca^{2+}-events might arise in the absence of intracellular Ca^{2+}-buffers during strong stimulation. Also N-type voltage sensitive Ca^{2+}-channels or cell type-specific Ca^{2+}-sensors with high and low

affinity might support prolonged presynaptic Ca^{2+}-signals. In MCs Ca^{2+}-influx through NMDA receptors channels might be involved (Chen et al., 2000b; Halabisky et al., 2000).

Experiments in brain slices demonstrated that the activation of GABA release from INs in the OB can depend on NMDA receptor input (Isaacson and Strowbridge, 1998; Schoppa et al., 1998). Glutamate release from MCs can cause long-lasting inhibitory GABA(A) receptor currents in the same MC even in the absence of action potential firing (Jahr and Nicoll, 1982; Isaacson and Strowbridge, 1998; Schoppa et al., 1998). In part, the long-lasting GABA release from INs appears to be triggered directly by Ca^{2+}-influx through the NMDA receptor (Chen et al., 2000a; Halabisky et al., 2000; Isaacson, 2001). Strong inputs to INs, in contrast, trigger Na^{+}- or Ca^{2+}-action potentials that invade large portions of the dendritic tree (Egger et al., 2005; Murphy et al., 2005; Zelles et al., 2006). Recent slice experiments indicated that GABA release from INs strongly depends on spike generation when background activity is introduced to approximate natural network dynamics (Schoppa, 2006b). This suggests, that feedback inhibition during odor processing in an intact network may not be dominated by a mechanism depending on NMDA receptors.

The experiments presented here can help to understand the relative contribution of local and lateral inhibition during an odor response in the intact system.

GABA(B) receptors mediated presynaptic inhibition of sensory input

GABA(B) receptors are mainly expressed in the glomerular layer (Bowery et al., 1987; Chu et al., 1990; Panzanelli et al., 2004) at the terminals of OSNs (Kratskin et al., 2006) where they inhibit transmitter release from OSN axon terminals and reduce stimulus evoked activity in the OB (Nickell et al., 1994; Wachowiak and Cohen, 1999b; Aroniadou-Anderjaska et al., 2000; McGann et al., 2005; Murphy et al., 2005; Wachowiak et al., 2005b; Vucinic et al., 2006). The density of GABA(B) receptors in deeper layers is very low (Bowery et al., 1987; Chu et al., 1990; Panzanelli et al., 2004). Nevertheless, GCs might be inhibited through GABA(B) receptors directly (Palouzier-Paulignan et al., 2002; Isaacson and Vitten, 2003). The presynaptic inhibition of OSN terminals via GABA(B) receptors might modulate the spatial and temporal pattern of activation across the array of glomeruli (Vucinic et al., 2006) and support slow temporal modulations of odor evoked responses in output neurons (Palouzier-Paulignan et al., 2002; Wilson and Laurent, 2005). It was also suggested that GABA(B) receptors plays a role for gain control, as they presynaptically control MC

excitation (Wachowiak et al., 2005a). However, the function of GABA(B) receptors during odor processing and their impact on OB output in an intact system is still not clear.

Objective of this thesis

The goal of this work was to examine the synaptic mechanisms underlying the spatio-temporal patterning of odor-evoked activity patterns in the intact OB of zebrafish. Odor responses of MCs and INs were measured using extra- and intracellular electrophysiological recordings and two-photon Ca^{2+}-imaging. To analyze the functional role of different synaptic interactions in an odor response, NMDA, AMPA, GABA(A) and GABA(B) receptors were manipulated pharmacologically. The results provide insights into the regulation of network excitability, receptor functions involved in neuronal synchronization and temporal modulation of MC odor responses.

Materials and Methods

Animals, preparation and odor stimulation

Zebrafish (Danio rerio) were kept at 26.5 °C at a day/night rhythm of 13/11 hours. Experiments were performed in an explant of the intact brain and nose (Friedrich and Laurent, 2001, 2004; Tabor et al., 2004). Adult zebrafish (>3 month old) were cold-anaesthetized, decapitated, and olfactory forebrain structures were exposed ventrally after removal of the eyes, jaws and palate. To optimize access of drugs, the dura mater over the ventro-lateral telencephalon close to the OB was removed with a fine forceps. Care was taken to avoid damage to the OB. The preparation was then placed in a custom made flow-chamber, continuously superfused with teleost artificial cerebro-spinal fluid (ACSF) (Mathieson and Maler, 1988), and warmed up to room temperature (~22 °C). All animal procedures were performed in accordance with the animal care guidelines issued by the Federal Republic of Germany.

Odors were applied to the nasal epithelium through a constant perfusion stream using a computer-controlled, pneumatically actuated HPLC injection valve (Rheodyne, Rohnert Park, CA, USA) as described in the literature (Friedrich and Laurent, 2001; Tabor et al., 2004). The volume of the applied solution and the flow rate were adjusted to obtain a stimulus duration of ~2.4 s. Stock solutions of amino acids (Fluka, Neu-Ulm, Germany) were made in distilled water at a concentration of 1 mM, stored at -18°C, and diluted in fresh ACSF to a final concentration of 10 µM immediately before the experiment. Extracts of commercially available dry fish food were prepared as described in the literature (Tabor et al., 2004) and kept at -6 °C for up to two weeks. Briefly, 200 mg of dry food was suspended in 50 ml of ACSF overnight, filtered through a filter paper and diluted 1:100 in ACSF immediately before the experiment. Different sorts of fish food were numbered arbitrarily. Food odor I was made from dry flake food, which was also used for daily feeding. Food odor III was made from dry bloodworms.

Pharmacological agents

Stock solutions of AP5 (10 mM in ACSF) and NBQX (1 mM in DMSO; both from Tocris Bioscience, Bristol, UK) were kept frozen and diluted 1:100-200 in ACSF immediately

before the experiment, yielding final concentrations of 5 – 10 µM NBQX and 50 – 100 µM AP5. Drug solutions were applied through the bath. In pilot experiments, effects of different drug concentrations between 50 – 500 µM AP5 and 5 – 50 µM NBQX were compared but no qualitative differences observed, indicating that drugs penetrated well into the tissue and produced maximal effects at the concentration used.

Stock solutions of [S-(R*,R*)]-[3-[[1-(3,4-Dichlorophenyl)ethyl]amino]-2-hydroxypropyl] (cyclohexylmethyl) phosphinic acid (CGP54626, 1 mM in ACSF, 2% DMSO), (R)-Baclofen (0.5 mM in ACSF) and SR 95531 hydrobromide (Gabazine, 25 mM in distilled and sterilized water; all from Tocris Bioscience, Bristol, UK) were kept frozen and further diluted in ACSF immediately before the experiment. Solutions were applied through the bath. In pilot experiments, different drug concentrations were tried. In all experiments concentrations were used, that showed clear effects: CGP54626 1-10µM, (R)-Baclofen 10-50µM and Gabazine 50-100µM.

Electrophysiological recordings

Electrophysiological recordings from MCs were performed in the ventro-lateral OB where amino acid-responsive neurons are located (Friedrich and Korsching, 1997; Friedrich and Laurent, 2001). Borosilicate patch pipettes (8 - 13 MΩ) were pulled on a P-2000 electrode puller (Sutter Instruments) and filled with intracellular solution containing (in mM): 130 K-gluconate, 10 Na-gluconate, 10 Na-phosphocreatine, 4 NaCl, 4 Mg-ATP, 0.3 Na-GTP, 10 HEPES (pH 7.25; ~300 mosm). Cells in the OB were visualized by differential interference contrast video microscopy or similar methods through a coverslip in the bottom of the chamber. Recorded neurons were selected for their large soma diameter (~10 µm) and a position close in the glomerular/MC layer. Anatomical studies demonstrated that these are characteristics of MCs (Edwards and Michel, 2002; Li et al., 2005; Fuller et al., 2006; Yaksi and Friedrich, 2006). Membrane potential values were corrected for a junction potential of -13 mV.

Recordings were performed using an Axoclamp 2B amplifier (Axon Instruments, Navato, USA) and digitized at 10 kHz using National Instruments hardware (National Instruments GmbH, Munich, Germany) and custom software written in IgorPro (Wavemetrics, Inc., Portland,USA). To prevent early clogging of the glass capillary tip, a pressure of ~100 mbar was applied to the pipette interior during penetration of the tissue and lowered to ~40 mbar before a target cell was approached. After formation of a Giga-seal and

break-in, intracellular whole-cell recordings were performed in current clamp mode (n = 35 MCs). In most cells, a small negative holding current was applied to stabilize recordings.

When Giga-seal formation or break-in could not be achieved, pipette pressure was released and extracellular recordings were performed in the loose-patch or cell-attached mode (n = 49 MCs). Two whole-cell recordings were lost during the experiment and continued as loose-patch recordings. Spontaneous firing rates of cells recorded in whole-cell mode (4.6 ± 3.8 Hz; mean ± SD) were slightly lower than those recorded extracellularly (7.6 ± 6.1 Hz), probably due to the holding current. When a recording was established, typically two food extracts and six amino acids were applied to select one or two stimuli that evoked a strong response in the recorded cell. These two stimuli were then applied two - eight times (normally five times) at 2 min intervals in a pseudo-randomly interleaved sequence, followed by ~15 min without odor stimulation to wash in drugs. The original stimulus sequence was then repeated. Completion of this stimulus protocol required continuous recordings for approximately 60 min. Recordings that were not stable up to this point, as judged by the measured resting potential and action potential amplitude, were excluded from the analysis. Drugs were then washed out for at least 30 min. When recordings were still stable, the stimulus sequence was repeated again. In total, responses of 74 neurons to 238 odor stimuli were measured before and during drug application, and 36 of these responses were tested again after wash-out.

To measure odor-evoked oscillatory activity in the LFP, glass micropipettes were filled with ACSF (8 – 13 MΩ) and positioned in the glomerular/MC layer. Recordings were made in bridge mode using an Axoclamp 2B amplifier (Axon Instruments) and band-pass filtered offline between 8 – 43 Hz. The position of the micropipette was optimized by small movements of the capillary tip while measuring oscillation amplitudes during stimulation with food extract.

Calcium Imaging

Two-photon Ca^{2+}-imaging

Two-photon Ca^{2+}-imaging experiments were performed in transgenic fish expressing yellow cameleon (YC) under the control of a fragment of the HuC promoter (HuC:YC) (Higashijima et al., 2003). In the adult OB, HuC:YC is expressed selectively in MCs (Li et al., 2005). HuC:YC-negative cells were collectively classified as INs and include periglomerular

and granule cells. YC fluorescence did not change in response to odor stimulation and was exclusively used as an anatomical marker.

The red-fluorescent Ca^{2+}-indicator, rhod-2-AM ester (Invitrogen, Karlsruhe, Germany), was injected into the OB as described previously (Yaksi and Friedrich, 2006). Briefly, 50 µg of rhod-2-AM was dissolved in 16 µl Pluronic F-127 (20% solution in DMSO, Invitrogen). This solution was then diluted 1:10 in ACSF before the experiment. The dye solution was loaded into a patch pipette after gently breaking off the very tip and pressure-injected into the OB under fluorescence optics. Injections were terminated when a predetermined fluorescence intensity level was reached to avoid excessive dye loading. To label MCs, multiple brief injections were made into the glomerular/MC layer at different sites. To label INs, injections were made into the granule cell layer. For details see Yaksi and Friedrich (2006).

Fluorescence images were acquired using a custom-built two-photon microscope (Wachowiak et al., 2004) equipped with a 20x water immersion objective (NA 0.95; Olympus, Hamburg, Germany). Two-photon fluorescence was excited at 830 nm by a mode-locked Ti:Sapphire laser (Mira900; 76 MHz; Coherent, Inc., Santa Clara, USA) pumped by a 10 W diode laser (Verdi; Coherent, Inc.). Fluorescence emission was detected externally by a photomultiplier-based whole-field detector in two wavelength channels (515/30 nm and 610/75 nm), allowing for the separate and simultaneous detection of HuC:YC and rhod-2 fluorescence, respectively. Image acquisition was controlled by custom software (CFNT; written by Ray Stepnoski at Bell Labs, Murry Hill, NJ, USA and Michael Müller at the Max-Planck-Institute for Medical Research, Heidelberg, Germany). Laser intensity was adjusted to minimize photobleaching.

To measure Ca^{2+} signals, series of images from a single focal plane were acquired at 128 ms/frame and 128 x 256 pixels or 256 ms/frame and 256 x 256 pixels. Previous experiments demonstrated that odor-evoked patterns of Ca^{2+} signals measured with this protocol are reproducible and stable over hours (Yaksi et al., 2007). To verify the stability of responses, the first stimulus was repeated least once in the sequence before the drug treatment was started, and typically multiple times during the initial phase of the experiment. When responses were not stable, experiments were discarded. Responses of INs were recorded in deep layers of the OB that contain predominantly granule cells. The focal plane was kept constant during an experiment. Slow drift was corrected if necessary using natural landmarks in the raw fluorescence image and in the HuC:YC fluorescence image.

Image series of raw rhod-2 fluorescence were converted into image series representing the fractional change in pixel intensity relative to a pre-stimulus baseline fluorescence (ΔF/F). Response maps were constructed by averaging ΔF/F images during a period of 5 s around response peak and mild spatial low-pass filtering using a Gaussian kernel (width, 5 pixels; σ, 1.2 pixels).

Conventional Ca^{2+}-imaging with a camera

Odor evoked activity in terminals of OSNs was visualized by fluorescence imaging with Calcium Green-1-dextran (10 kD; Invitrogen) as described in the literature (Friedrich and Korsching, 1997). In order to fill neurons, fish were anesthetized with 0.01% MS-222 and about 1 µl of a staining solution, containing 6 – 8 % Calcium Green-1-dextran in 3 mM NaCl and 0.1 % Triton X-100, was injected into each naris. After 5 min the solution was washed away and fish were allowed to recover from anaesthesia. Triton X-100 permeabilized the membrane of olfactory cilia to allow the dye uptake into the neurons. Cilia regenerate during 48 hr (Friedrich and Korsching, 1997). After 3-6 d of recovery fish were used for imaging experiments.

Odor responses from OSN terminals were viewed with a custom-made upright epifluorescence microscope equipped with a BX-RFA epifluorescence condenser (Olympus), a 40 x water immersion objective (NA 0.95; Olympus) and a high speed, low-noise CCD camera (NeuroCCD-SM; 80 x 80 pixels, 14 bits; RedShirtImaging, LLC, Decatur, USA). Fluorescence was excited with a 150 W Xe arc lamp equipped with a stabilized power supply (Opti-Quip, Highland Mills, USA) through an excitation filter (bandpass 485/20). Light was attenuated to 1.5 % of the full intensity by neutral density filters to minimize photobleaching. Excitation filter, dichroic mirror and emission filters used were 485 ± 20 nm, 510 nm and 515 nm (long-pass) or 540 ± 25 nm, respectively. Series of images (80 x 80 pixels, 14 bits) were recorded at 40 - 500 Hz and binned temporally to a final frame interval of 2 – 200 ms. Stimuli were presented two or three times and image series were averaged.

Image series were processed as described for two-photon-imaging.

Data analysis

Data were analyzed off-line using routines written in Igor pro (Wavemetrics, Inc., Portland, USA) or MATLAB (Mathworks, Inc., Natick, USA). Trains of APs were described

as series of delta functions and convolved with a Gaussian kernel (σ, 200 ms; other values gave similar results) to obtain firing rate functions. Firing rate functions from repeated stimulus applications (3 – 8 repetitions per stimulus, usually ≥ 5) were averaged, yielding PSTHs. As the flow rate was not absolutely constant throughout the experiments and across experiments, the response onset was defined at the beginning of increased or decreased firing about 2 seconds after switch of the odor valve. The earliest event across all individual odor presentations was considered as odor stimulus onset. Spontaneous firing rates were measured during the 2 s - prestimulus period and/or in recordings without stimulation. Action potentials and the time intervals considered per individual cell (usually > 10 s) were summed up and used to calculate the average firing rate. Effects of drugs on odor responses were assessed by subtracting PSTHs measured in the presence of a drug from PSTHs measured before drug application in response to the same odors.

Mean response amplitudes of single neurons measured under different conditions were compared using a paired Student's t-test because measurements of responses from individual neurons in repeated trials were approximally normally distributed. Mean responses across population of neurons were usually not normally distributed and compared using a non-parametric sign test. To test for statistical differences between correlation strengths, correlation coefficients were transformed using the Fisher Z transform and compared using the z statistic.

Results

Pharmacological investigation of GABA receptor function in the olfactory bulb

To examine the role of GABAergic interactions on odor-evoked activity patterns in the OB I first pharmacologically manipulated GABA receptors in an explant of the entire brain and nose of adult zebrafish. I investigated presynaptic glomerular activity patterns by Ca^{2+}-dependent imaging with a camera, evoked oscillations in the field potential measured by electrodes and MC responses by loose-patch extracellular and whole-cell intracellular recordings. Odor stimuli included food extracts and amino acids. Amino acids are natural odors for aquatic animals and were used at a concentration (10 μM) that is in the intermediate physiological range and does not saturate glomerular odor responses in zebrafish (Friedrich and Korsching, 1997). GABA(B) receptors were activated using the selective agonist, baclofen (10 – 50 μM), and inhibited using the selective antagonist, CGP54626 (1 – 10 μM). GABA(A) receptors were inhibited using the selective antagonist, Gabazine (50 – 100 μM). Unless otherwise noted, spontaneous activity and odor responses were first measured in the absence of drugs. Drugs were then washed in through the bath for at least 10 min and responses to the same set of odors were measured again. When recordings were stable for an extended period of time, drugs were washed out for at least 30 min and odor responses were measured again.

Presynaptic inhibition of olfactory sensory neuron terminals by GABA(B) receptors

In various vertebrate and invertebrate species, the activation of GABA(B) receptors on OSN axon terminals decreases presynaptic Ca^{2+}-influx and thereby attenuates the release of glutamate during an odor response (Wachowiak and Cohen, 1999b; Aroniadou-Anderjaska et al., 2000; McGann et al., 2005; Murphy et al., 2005; Wachowiak et al., 2005b; Vucinic et al., 2006). In order to examine whether GABA(B) receptors mediate a similar effect in zebrafish, I loaded OSNs with the fluorescent Ca^{2+}-indicator, Calcium Green-1 dextran, and measured odor-evoked Ca2+ signals in OSN axon terminals. In control experiments, odors evoke specific patterns of fluorescence changes in the OB, reflecting patterns of sensory input across the array of glomeruli (Friedrich and Korsching, 1997).

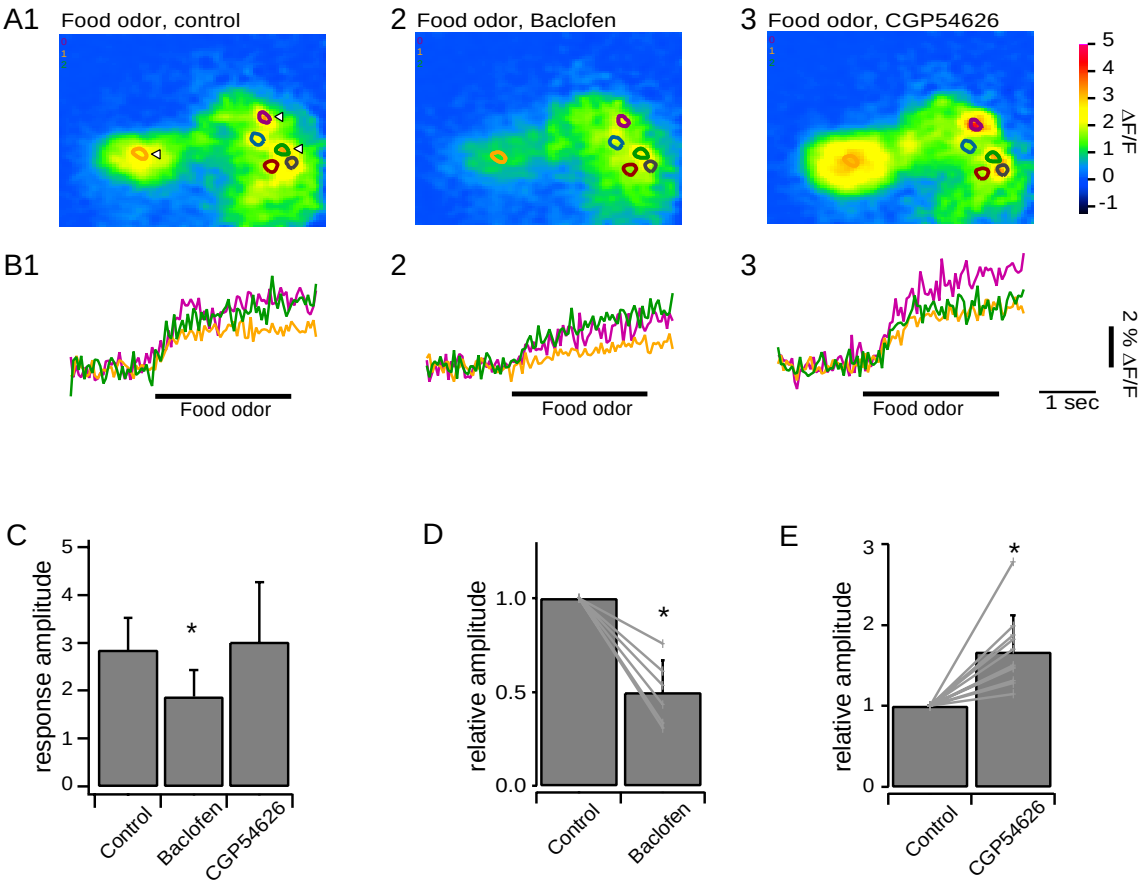

Figure 2. GABA(B) receptors modulate odor evoked signals in OSN terminals. (A) Presynaptic glomerular calcium signals evoked by food odor stimulation and measured by Calcium Green-1-dextran (A1) before drug application, (A2) after wash in of Gabazine, (A3) and after rinsing and wash in of CGP54626 in the same fish. (B) Time course of the calcium signal averaged over pixels in three regions indicated by arrowheads in (A). (B1) Before drug application, (B2) after wash in of Gabazine, (B3) and after rinsing and wash in of CGP54626. (C) Response amplitudes averaged over six regions indicated by circles before drug application, after wash in of Gabazine and after rinsing and wash in of CGP54626. Error bars show SDs. Star indicates change relative to control significant with $p<0.04$ (sign test). (D) Effect of Baclofen for 3 experiments and 6 odors. Response amplitudes are normalized to control. Individual changes are indicated by lines. Bars and error bar show average and SD. Star indicates change significant with $p<0.04$ (sign test). (E) Effect of CGP54626 for 6 experiments and 11 odors. Response amplitudes are normalized to control. Individual changes are indicated by lines. Bars and error bar show average and SD. Star indicates change significant with $p<0.01$ (sign test).

In the presence of baclofen or CGP54626, the spatial distribution of odor-evoked Ca^{2+}-signals was similar to control. However, baclofen significantly reduced the amplitude of Ca^{2+}-signals (n = 6 odors in 3 OBs; mean ± SD: 49 ± 17 % of control; Student's t-test: P = 0.01; Fig. 2A-D) while CGP54626 enhanced them (n = 11 odors in 6 OBs; 167 ± 46 % of control; mean ± SD; Student's t-test_ P = 0.005; Fig. 2A - C, E). These effects of baclofen and CGP54626 were observed in all experiments. Hence, GABA(B) receptors attenuate Ca^{2+}-influx in OSN axon terminals during an odor response, consistent with reports from other species.

Effect of GABA(B) receptor blockade on mitral cell odor responses

To investigate how GABA(B) receptors influence the output activity of the olfacory bulb, I examined the effect of the GABA(B) receptor antagonist, CGP54626, on spontaneous and odor-evoked activity of MCs (n = 20 odor responses from 11 MCs). CGP54626 did not significantly change the average spontaneous firing rate of MCs (n = 11 MCs; control: 7.0 ± 3.9 Hz, mean ± SD; CGP54626: 7.5 ± 4.3 Hz; sign test: P = 0.6) and caused no obvious changes in subthreshold membrane potential fluctuations (Fig. 3A).

The effects of CGP54626 on odor evoked responses were heterogeneous (Fig. 3B). In 11 out of 20 cases, CGP54626 caused no obvious effect on the amplitude or time course of the response. In the remaining 9 responses, the amplitude was decreased by CGP54626 in two cases and increased in 7 cases. In 4 out of the 9 responses, the change in response amplitude was nearly constant throughout the course of the odor response. As a consequence, the time course of the response remained similar to control. In the remaining 5 responses, CGP54626 changed response amplitude during specific epochs of the response and, hence, changed the time course (Fig. 3B2, B4). Effects of CGP54626 were at least partially reversible after washout.

Response amplitudes reach their maximum usually during the first second after odor onset and were quantified in the interval from 0.25 to 0.75 s. On average, odor stimulation increased MC firing rates under control conditions by 8.4 ± 16.1 Hz (mean ± SD; n = 20 responses). In the presence of CGP54626, the average response amplitude was not significantly changed (9.8 ± 15.9 Hz; sign test: P = 0.8; Fig. 4A) and the cumulative distribution of response amplitudes remained similar (Fig. 4B).

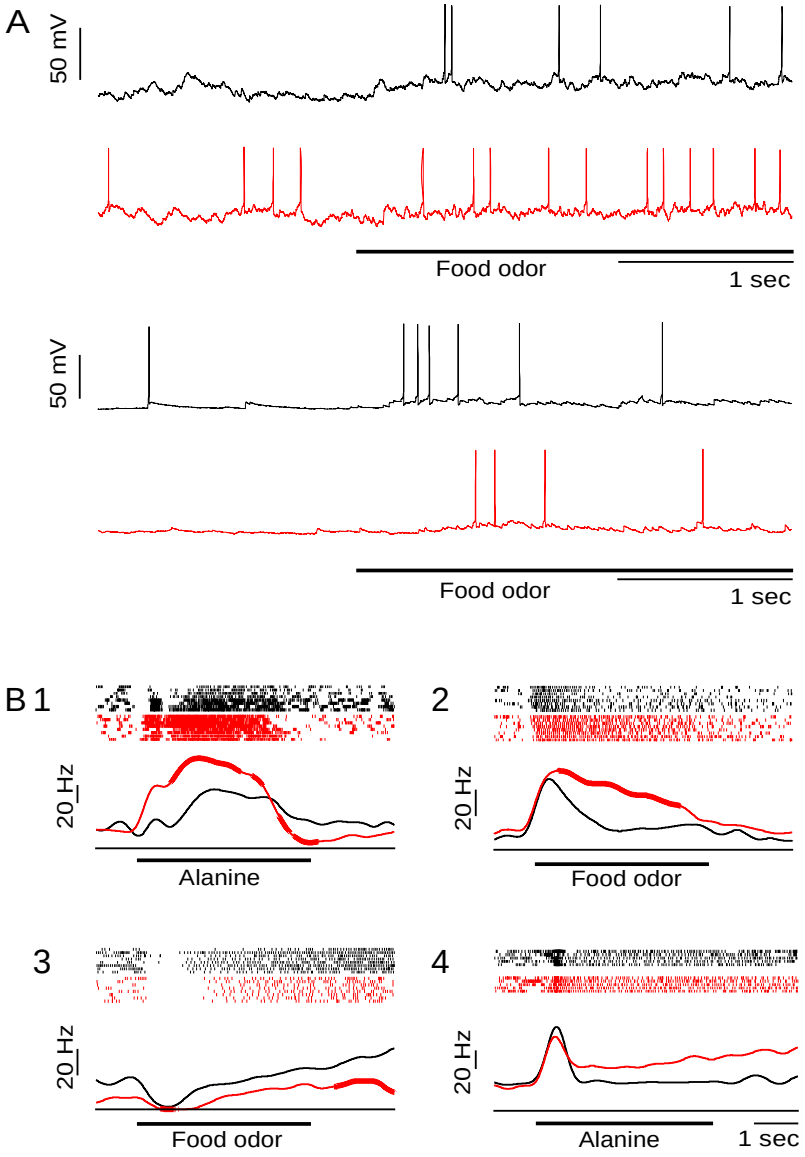

Figure 3. Effect of the GABA(B) antagonist, CGP54626, on odor responses of MCs. (A) Whole-cell recordings of food odor responses from two MCs (thick bar indicates stimulus) before (black) and during (red) bath-application of the drug. (B1 – B4) Four examples illustrating effects of CGP54626. Ticks denote individual action potentials. Each row shows one trial. Black: control; red: CGP54626 application. Continuous lines are PSTHs, averaged over all trials under each condition. Thick portions depict time bins where PSTHs were significantly different (Student's t-test; $P < 0.05$) from the corresponding time bin in the control PSTH (black).

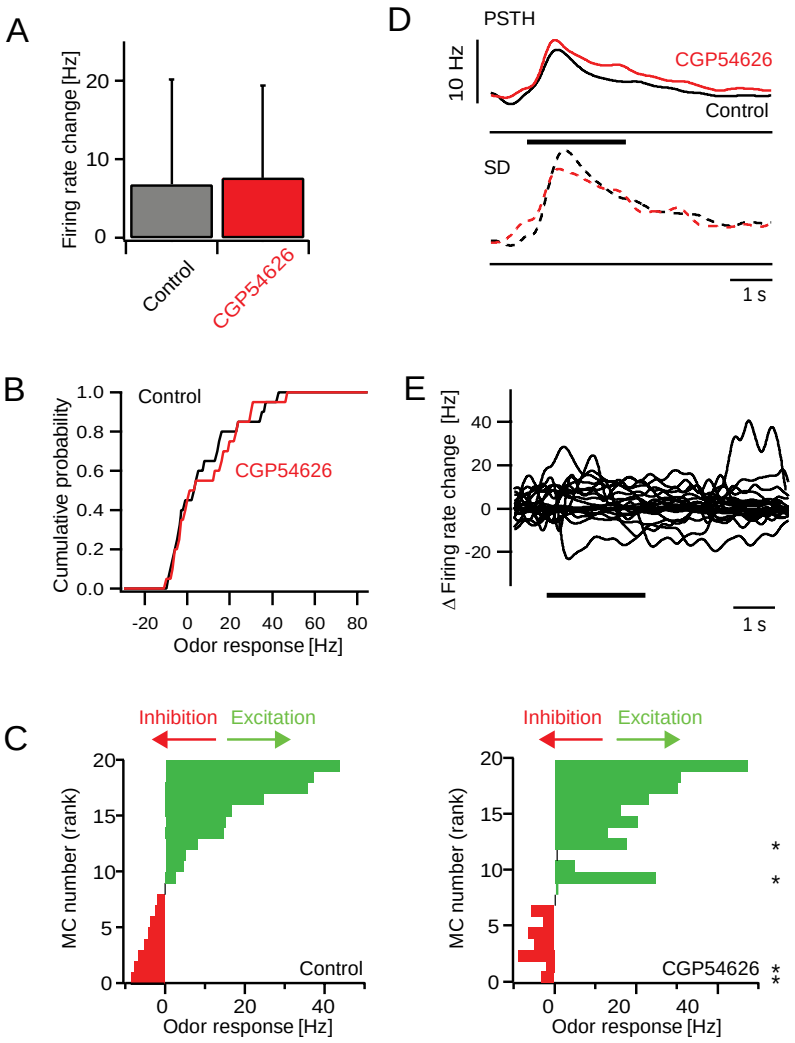

Figure 4. Effect of CGP54626 on odor responses of MCs: quantitative analysis. (A) Mean firing rate change evoked by odor stimulation before (control) and during CGP54626 treatment in the time window between 0.25 and 0.75 s after response onset. Error bars show SD. P = 0.5 (sign test). (B) Cumulative distribution of odor-evoked firing rate changes in MCs before (control) and during drug application. (C) Left: MC odor responses ranked according to the firing rate change measured before application of CGP54626. Right: Responses of the same MCs to the same odors in the presence of the drug (same rank order as control). Asterisks denote responses that were significantly changed (Student's t-test; $P < 0.05$). (D) Top (continuous lines): average PSTH of MC odor responses before (control) and during CGP54626 treatment. Dashed lines show SD (bottom). (E) Differences of PSTHs (CGP54626 – control) for all MC odor responses.

Because CGP54626 had heterogeneous effects on individual odor responses, I visualized the individual effects of CGP54626 by ranking recorded responses according to their amplitude under control conditions (Fig. 4C). Although some response amplitudes in the presence of CGP54626 were significantly different from control, the pattern of response amplitudes remained relatively similar. On average firing frequencies were slightly, though not significantly increased throughout the whole time course of the odor response, as visible in the averaged PSTHs (Fig. 4 D). The effect of CGP54626 on the time course of individual odor responses was visualized by subtraction of the PSTH of an odor response measured under control condition from the corresponding PSTH measured in the presence of CGP54626. Individual changes were mostly long-lasting but often small (Fig. 4 E). Hence, the blockade of GABAB receptors had little or no effect on the mean amplitude of MC responses but caused a slight reorganization of odor-evoked activity patterns across the MC population.

Effect of GABA(A) receptor blockade on mitral cell odor responses

Next, I studied the effect of GABA(A) receptor blockade on MC activity using Gabazine (29 odor responses measured in 19 MCs). On average, Gabazine significantly increased the spontaneous firing rate (control: 4.2 ± 4.9 Hz, Gabazine: 8.5 ± 6.5 Hz, sign test: $P = 0.001$). In individual MCs, spontaneous firing was either similar to control or increased, while decreased spontaneous firing was never observed. Moreover, in 7/20 MCs, the pattern of spontaneous action potential firing changed from irregular firing under control conditions to burst firing in the presence of Gabazine.

In the presence of Gabazine all neurons were still responsive to odor stimulation (Fig. 5). Evoked firing rates were usually much higher than in the control measurements. Particularly transiently increased firing rates immediately after odor onset were drastically amplified. Responses that were dominated by inhibition under control conditions became excitatory in 2/8 cases. In the remaining 6 cases, however, inhibitory response epochs were still observed in the presence of Gabazine. In the presence of Gabazine, many odor responses started with a high-frequency burst of firing, followed by a period of silence. Thereafter, MCs often fired a series of bursts at a frequency of about 1 Hz. For a given MC and stimulus, these firing patterns were at least partially reproducible in successive trials and therefore apparent in averaged PSTHs (Fig. 5 B1, B3, B4).

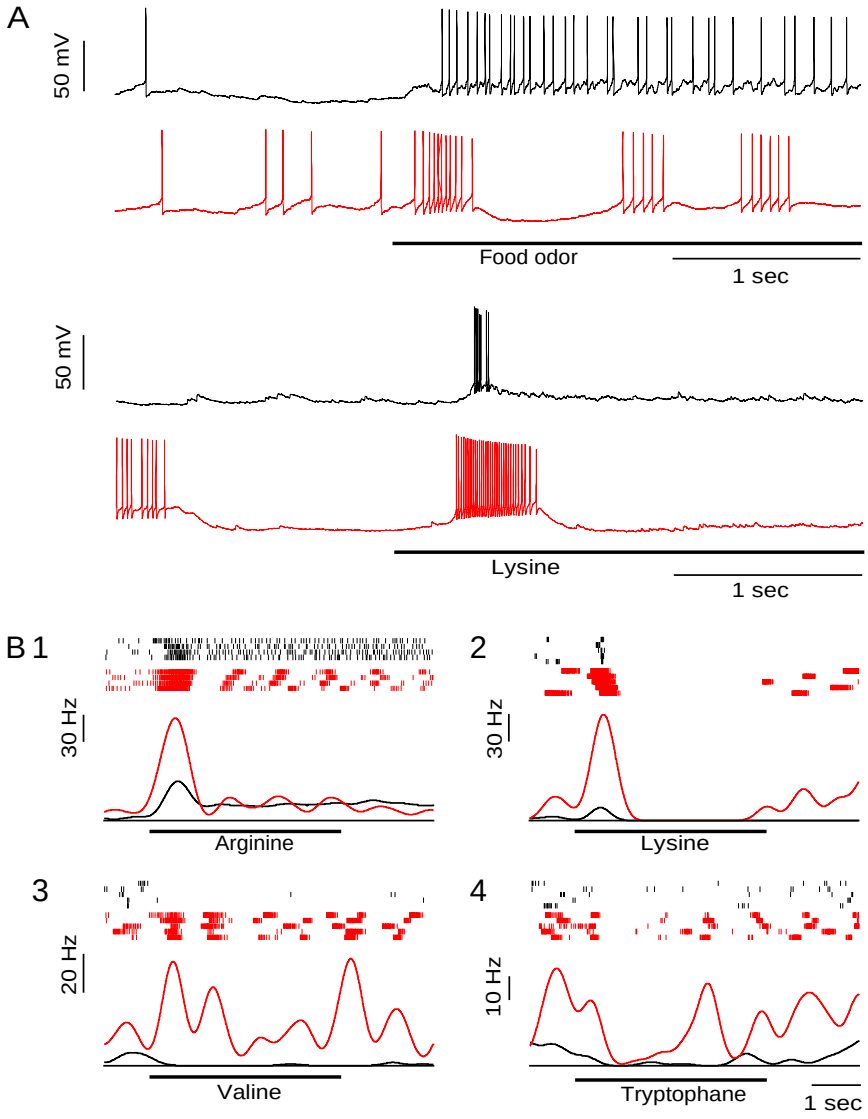

Figure 5. Effect of the Gabazine on odor responses of MCs. (A) Whole-cell recordings of responses from two different MCs before (black) and during (red) bath-application of the drug. Thick bar indicates stimulus. (B1 – B5) Four examples illustrating the effects of Gabazine. Conventions as in Fig. 3. Responses are from different cells and were recorded in the whole-cell, cell-attached or loose-patch configuration.

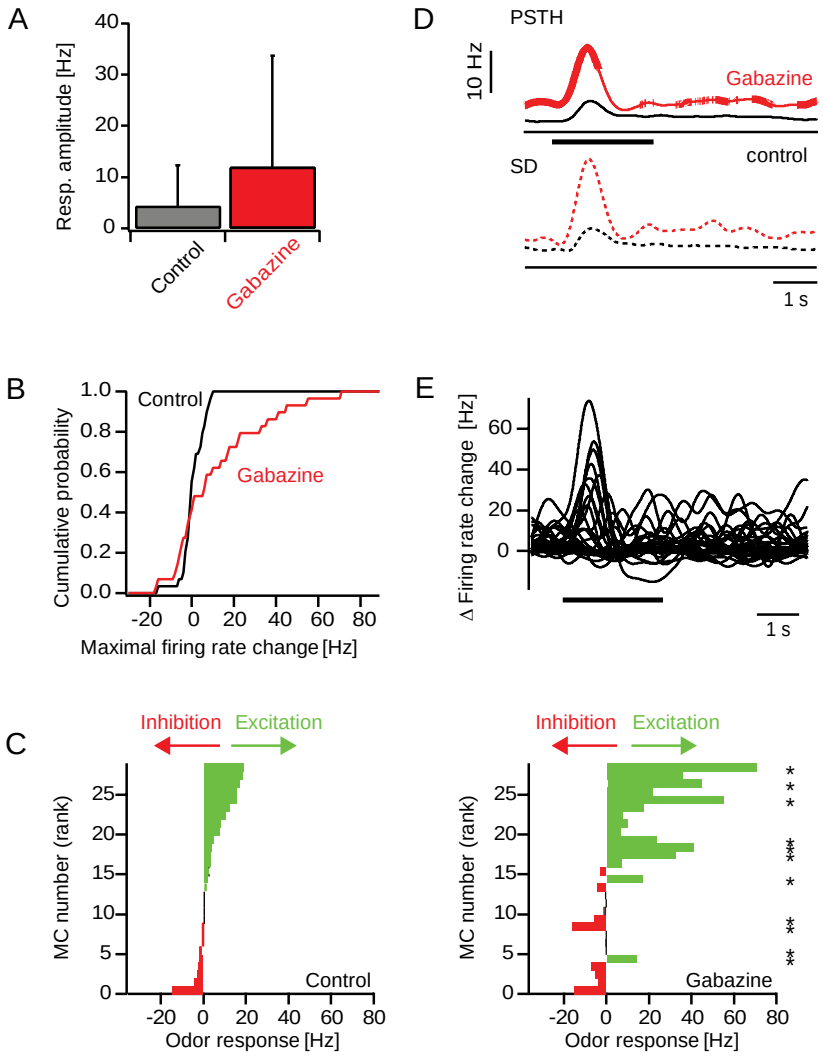

Figure 6. Effect of Gabzine on odor responses of MCs: quantitative analysis. (A) Mean firing rate change evoked by odor stimulation before (control) and during Gabazine treatment in the time window between 0.25 and 0.75 s after response onset. Error bars show SD. P = 0.46 (sign test). (B) Cumulative distribution of odor-evoked firing rate changes in MCs before (control) and during drug application. (C) Left: MC odor responses ranked according to the firing rate change measured before application of Gabazine. Right: Responses of the same MCs to the same odors in the presence of the drug (same rank order as control). Asterisks denote responses that were significantly changed (Student's t-test; $P < 0.05$). (D) Top (continuous lines): average PSTH of MC odor responses before (control) and during Gabazine treatment. Thick portions depict time bins where the PSTH was significantly different from control (sign test; $P < 0.05$). Dashed lines show SD (bottom). (E) Differences of PSTHs (Gabazine – control) for all MC odor responses.

The average response amplitude between 0.25 and 0.75 s after onset was enhanced in the presence of Gabazine (control: 5.9 ± 10.7 Hz; Gabazine: 13 ± 23.3 Hz; Fig. 6 A). Even though this effect appeared pronounced, it was not statistically significant (sign test: P = 0.5), presumably because the magnitude of inhibitory responses was also increased due to the elevated spontaneous firing rate. The cumulative distribution of odor-evoked firing rate changes shows that strong excitatory responses became more frequent in the presence of Gabazine (Fig. 6 B). The pattern of recorded response amplitudes was substantially different from control (Fig. 6 C). The average PSTH and the analysis of individual responses revealed that Gabazine substantially increases the average MC firing rates particularly during the initial phase of the odor response (Fig. 6 C), consistent with the frequent occurrence of high-frequency bursts shortly after response onset. However, MC firing rates were also significantly increased during later response phases and during spontaneous firing (before stimulus onset; Fig. 6 E). These data indicate that GABA(A)-mediated inhibition regulates MC firing rates during spontaneous and odor evoked activity.

During treatment with Gabazine odor stimulation usually evoked rhythmical bursting with a frequency around 1 Hz (Fig. 5A1, B1, B3 + Fig. 7). This periodicity is at least loosely time-locked to odor onset and also visible in the averaged odor response of individual odor responses (Fig. 5B1 + B3) but the exact frequencies can vary among responses to different odors. An analysis of the Power spectral density shows a peak at 1Hz that is not present under control conditions. This indicates that blockade of GABA(A) receptors cause slow rhythmic bursting which is reminiscent of epileptic activity.

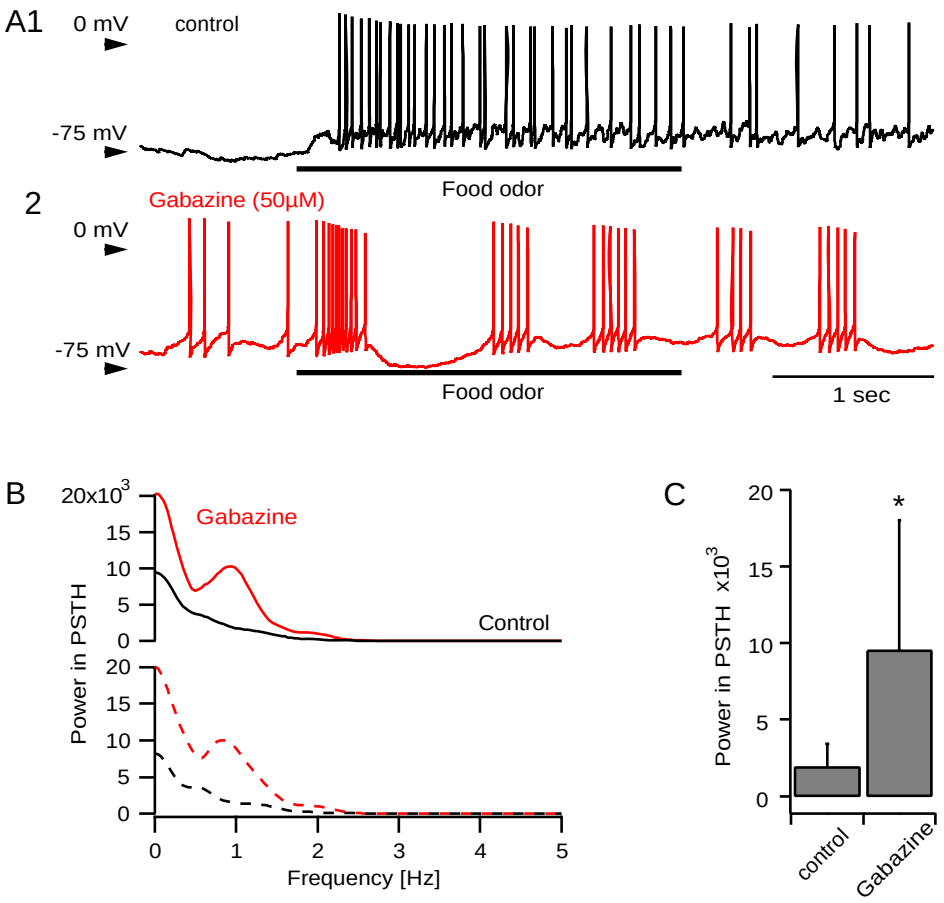

Figure 7. Periodic activity in MC odor responses induced by Gabazine. (A) Whole-cell recording of a MC response to food odor stimulation before and during treatment with Gabazine. Bar indicates stimulus. (B) Average (solid line) and SD (dashed line) of power spectra derived from PSTHs of 29 experiments during a four seconds window starting 1 second after stimulus onset. Black: control; Red: Gabazine. (C) Average power from PSTHs of 29 experiments calculated from 0.8 to 1.2 Hz before and during Gabazine treatment. Error bars show SD. Star indicates statistically significant change ($P < 0.001$ t-test)

Effect of GABA(A) receptor blockade on odor evoked oscillations in the local field potential

Previous studies indicated that GABAergic feedback at the reciprocal synapse between MCs and local INs is involved in the synchronization of output neurons (Nusser et al 2001, Friedman and Strawbridge 2003, Lagier et al 2004). In zebrafish odor stimulation reliably evokes 20 Hz oscillations in the LFP. To investigate whether GABA(A) receptors are involved in this synchronization the effect of Gabazine on LFP oscillations was analyzed. A blockade of GABA(A) receptors lead to a complete loss of fast odor evoked oscillations (Fig. 8 B). Instead low frequency oscillations of about 1Hz appeared when no odor stimulus was present but vanished after stimulus onset (Fig. 8 A). The Fast Fourier Transformation reveals a clear peak at about 20 Hz during odor stimulation that is abolished by Gabazine.

These data show that synaptic interactions mediated by GABA(A) receptors are necessary for odor evoked network oscillations and indicate that fast inhibitory feedback also suppresses spontaneously synchronized network activity.

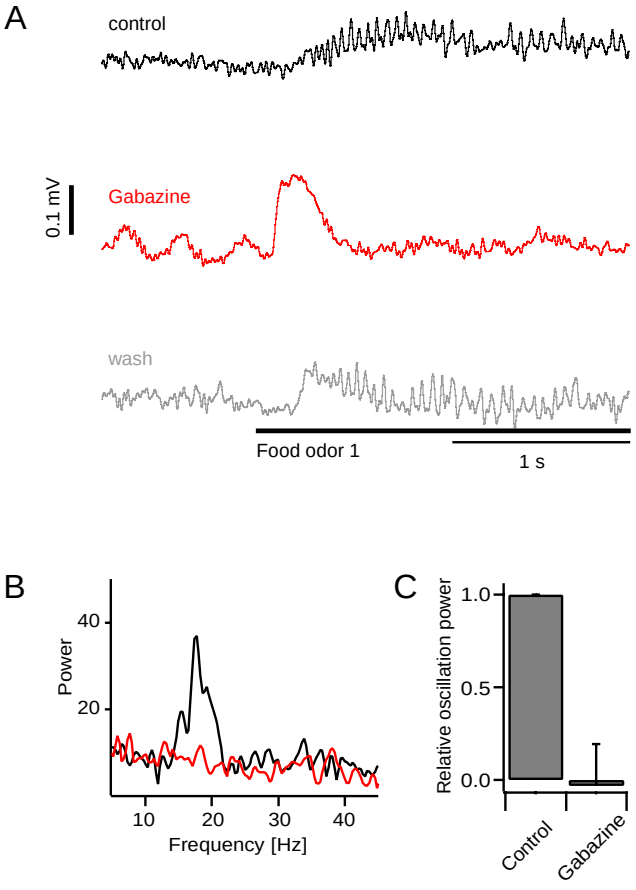

Figure 8. Effect of Gabazine on oscillations in the LFP. (A) Recording of odor evoked activity in the LFP before (black) and during application of Gabazine (red) and after wash-out (grey). Traces were filtered by a 40 Hz lowpass filter and corrected for slow drifts by subtraction of a box car smoothed (box width 1 s) average of nine individual recordings. Bar indicates stimulus. (B) Power spectral density of odor evoked oscillations and averaged over trails from one experiment before and during application of Gabazine. (C) Power in the frequency band from 15 to 30 Hz normalized to control and averaged over 5 experiments before and during Gabazine treatment. Error bars show SD. Star indicates statistically significant change. $P < 0.001$ (t-test)

Pharmacological investigations of ionotropic glutamate receptor function in the olfactory bulb

I pharmacologically manipulated AMPA receptor and NMDA receptor function using the selective antagonists NBQX (5 – 10 μM) and AP5 (50 – 100 μM), respectively. I first measured the effect on odor responses of MCs by loose-patch extracellular and whole cell intracellular recordings.

Combined blockade of AMPA receptors and NMDA receptors

First, I blocked all iGlu receptors with NBQX and AP5. In the presence of NBQX and AP5, spontaneous AP firing was either completely abolished or became slow and periodic (n = 4 MCs; Fig. 9A). Sub-threshold membrane potential fluctuations were reduced or eliminated and spontaneous fluctuations in the LFP were decreased (Fig. 9A, B). Odor stimulation failed to elicit MC depolarization and action potential firing (3 amino acid odors and 3 food extracts tested; 1 – 2 stimuli per MC; Fig. 9A). Moreover, odor-evoked LFP oscillations were completely abolished (n = 6 stimuli in 4 OBs; 4 ± 1 % of control power in 15 – 30 Hz band; t-test: $P < 0.001$; Fig. 9B, C, D). These results show that glutamatergic synaptic transmission is essential for responses of OB neurons to odors, most likely because glutamate is the neurotransmitter of OSNs (Berkowicz et al., 1994; Ennis et al., 1996).

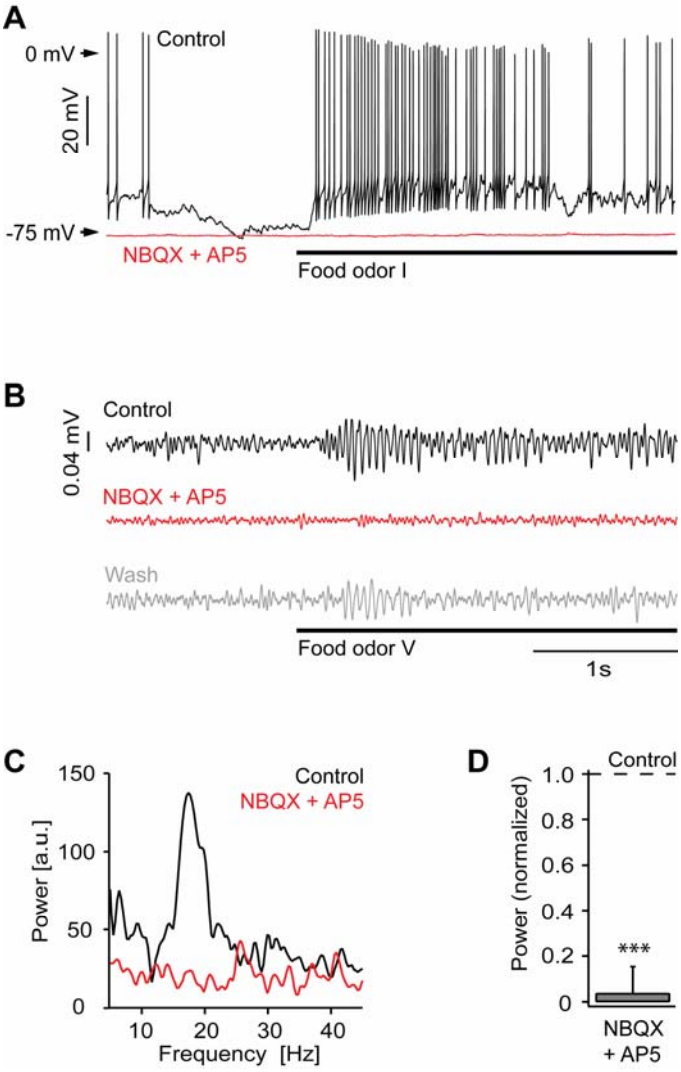

Figure 9. **iGluRs are essential for odor responses of MCs.** (A) Whole-cell recording from a MC during odor stimulation (food extract; bar) before (black) and during (red) application of NBQX and AP5. (B) LFP recording during odor stimulation (food extract; bar) before (black), during (red) and after (gray) application of NBQX and AP5. Traces are band-pass filtered between 8 – 43 Hz. (C) Power spectra of LFP traces (average of 6 trials; from unfiltered data) for the examples shown in (B). (D) Average LFP power (15 – 30 Hz) in the presence of NBQX and AP5, normalized to control (n = 4 OBs). ***, $P < 0.001$ (t-test) (Tabor and Friedrich, 2008)

Blockade of AMPA receptors: effect on mitral cell responses

In contrast to the combined application of AMPA receptor and NMDA receptor antagonists, the selective blockade of AMPA receptors by NBQX produced diverse effects on MC activity. The spontaneous activity of individual MCs could decrease, remain similar, or even increase relative to control levels. On average, NBQX did not significantly change the spontaneous firing rate (control: 6.6 ± 3.61 Hz; NBQX: 5.51 ± 4.90 Hz; mean ± SD; sign test: $p = 0.23$; $n = 13$ MCs). Sub-threshold activity was analyzed in six mitral cells. In five of these cells steep subthreshold transients in the membrane potential were strongly reduced while slow fluctuations could still be observed (Fig. 10A).

All MCs were still odor-responsive in the presence of NBQX ($n = 22$ odor responses in 13 MCs; 1 – 3 different odors per MC), but the magnitude and time course of odor responses was usually altered (Fig. 10 A, B). Paradoxically, NBQX often enhanced transient periods of excitation shortly after response onset (Fig. 3B1 – B3), while reductions in the amplitude of excitatory responses were rare. Inhibitory responses were prolonged in two cases (Fig. 10 B4) and unchanged in one case. In two other cases, the sign of the response changed from an inhibition to a weak excitation (Fig. 10 B5). In both of these cases, NBQX almost completely suppressed spontaneous activity. Changes in the sign of the response from excitatory to inhibitory were not observed. The effects of NBQX were at least partially reversed after wash-out.

To quantify the effects of NBQX on odor responses I first compared the average odor-evoked firing rate change before and during NBQX treatment between 0.25 and 0.75 s after response onset. On average, odor stimulation evoked an increase in MC firing under control conditions (4.0 ± 9.7 Hz above baseline) that was significantly enhanced by NBQX (11.5 ± 18.9 Hz; sign test: $P = 0.02$; Fig. 11 A). The cumulative distribution of response amplitudes was shifted to the right and saturated at higher frequencies (Fig. 11 B), showing that smaller responses became less frequent and maximal response magnitudes were increased. However, not all responses were enhanced by NBQX and the effect of NBQX depended on the neuron and stimulus, suggesting that NBQX may also affect the pattern of activity across the population of MCs. I therefore compared responses of different MCs to different odors before and during application of NBQX in a diagram where responses are ranked according to the response magnitude before drug application (Fig. 11 C). Response patterns before and during application of NBQX showed obvious similarities, indicating that NBQX did not cause major changes in population activity patterns. Nevertheless, many, but not all, responses in the

presence of NBQX were significantly different from control. Thus, the blockade of AMPA receptors not only scaled odor responses but also caused small changes in the distribution of activity across the MC population.

To assess the effect of NBQX on the time course of MC responses in more detail, I constructed PSTHs. The enhancement of the mean response of MCs was most pronounced during the early phase of the odor response (Fig. 11 D). The effect of NBQX on individual responses was examined by subtracting the PSTH measured before NBQX treatment from the corresponding PSTH measured in the presence of NBQX (Fig. 11 E). This analysis confirmed that NBQX increased odor responses in a subset of MCs, particularly during the initial phase of the odor response, while suppressive effects of NBQX were small.

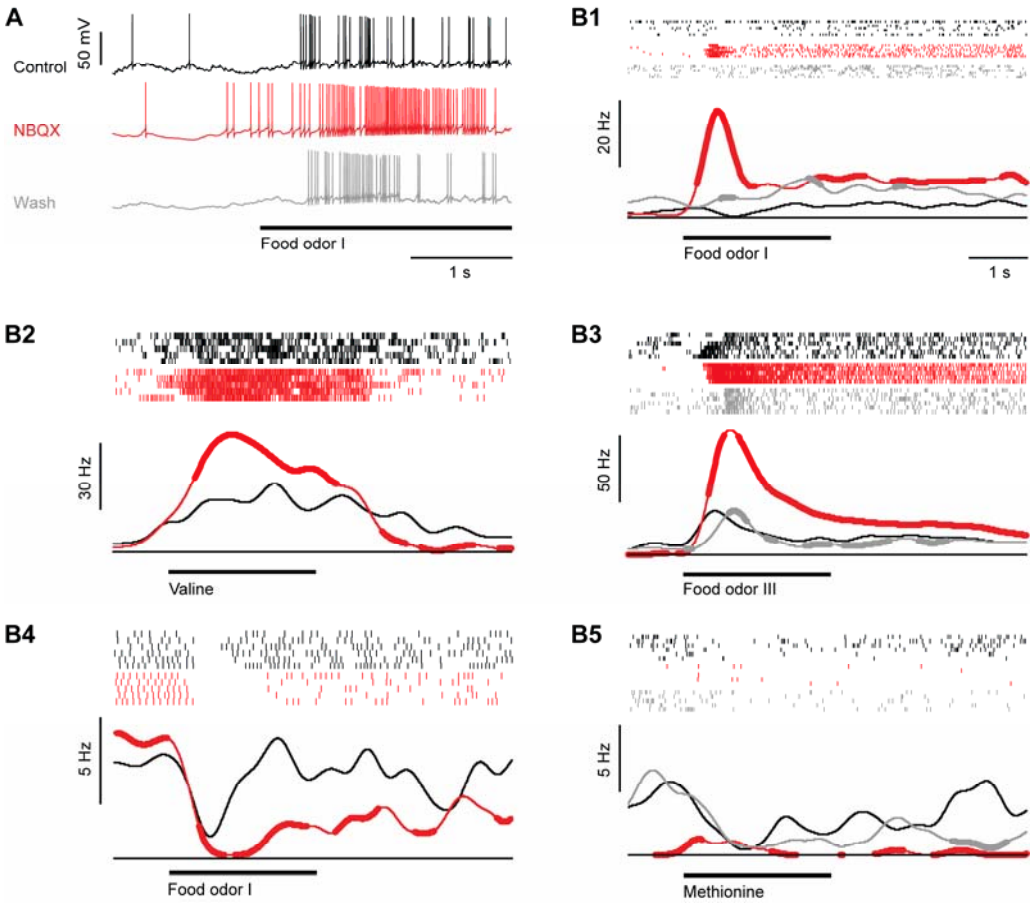

Figure 10. Effect of the AMPA receptor antagonist, NBQX, on odor responses of MCs. (A) Whole-cell recording of a MC response to odor stimulation before (black), during (red) and after (gray) bath-application of NBQX. Thick bar indicates odor stimulus. (B1 – B5) Five examples illustrating effects of NBQX on odor responses. Conventions as in Fig. 3. Responses are from different cells and were recorded in the whole-cell, cell-attached or loose-patch configuration. (Tabor and Friedrich, 2008)

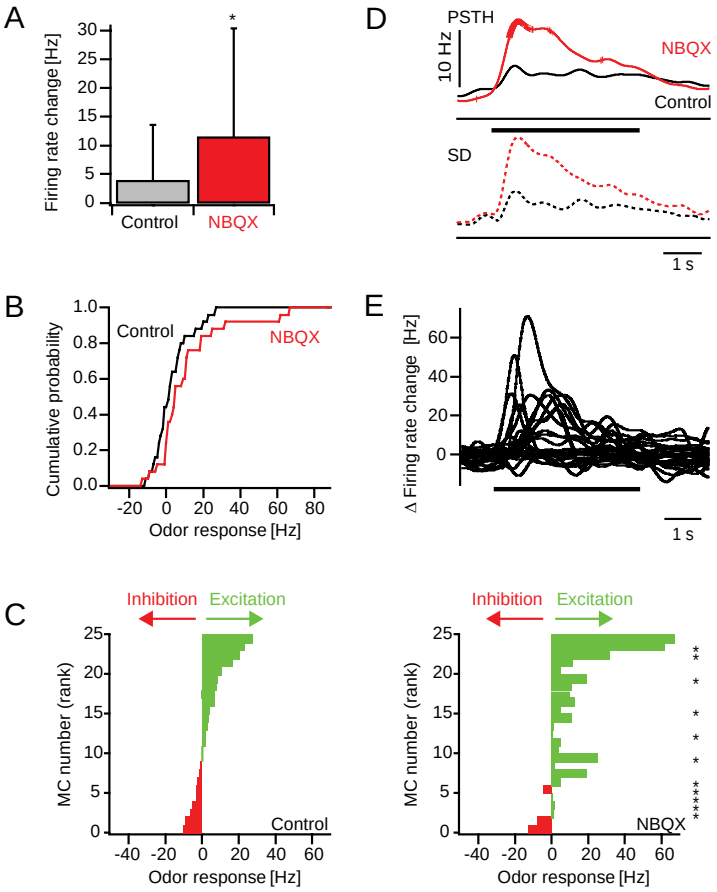

Figure 11. Effect of NBQX on odor responses of MCs: quantitative analysis. (A) Mean firing rate change evoked by odor stimulation before (control) and during NBQX treatment in the time window between 0.25 and 0.75 s after response onset. Error bars show SD. *, P = 0.02 (sign test). (B) Cumulative distribution of odor-evoked firing rate changes in MCs before (control) and during NBQX application. (C) Left: MC odor responses ranked according to the firing rate change measured before NBQX application. Right: Responses of the same MCs to the same odors in the presence of NBQX (same rank order as control). Asterisks denote responses that were significantly changed in the presence of NBQX (Student's t-test; $P < 0.05$). (D) Top (continuous lines): average PSTH of MC odor responses before (control) and during NBQX treatment. Thick portions depict time bins where the PSTH was significantly changed (sign test; $P < 0.05$). Dashed lines show SD. (E) Differences of PSTHs (NBQX – control) for all MC odor responses. (Tabor and Friedrich, 2008)

Blockade of NMDA receptors: effects on mitral cell responses

The selective blockade of NMDA receptors by AP5 had little effect on spontaneous MC activity. In one MC, spontaneous AP firing was completely abolished, while it was slightly increased in others. On average, spontaneous firing rates in the presence of AP5 were not significantly different from control (control: 8.6 ± 6.5 Hz, AP5: 9.4 ± 7.2 Hz, sign test: P = 1.00; n = 12 MCs) and fluctuations in the membrane potential appeared largely unchanged (Fig. 12 A).

Odor responses were still observed after AP5 treatment in all recorded neurons (n = 25 responses from 12 MCs; 1 – 3 different odors per MC), but the amplitude and time course were often changed (Fig. 12 A, B). The effects caused by AP5 appeared more complex than those caused by NBQX. While excitatory response amplitudes were often slightly increased by AP5 (Fig. 12 B2-B4), decreases in response amplitude were also observed (Fig. 12 A, 5B1). In some neurons, AP5 affected mainly the initial response transients (Fig. 12 B4) whereas in others it changed the later response phases (Fig. 12 B1, B2, B3, B5). Changes in the sign of the response amplitude were observed in 4 out of the 25 responses. In one case, a weak inhibitory response became excitatory while in the other three cases excitatory responses became inhibitory (Fig. 12 A, B1). Effects of AP5 were at least partially reversible after washout.

In the presence of AP5, the average firing rate change of MCs between 0.25 and 0.75 s was not significantly different from control (control: 5.0 ± 15.7 Hz ; AP5: 8.5 ± 20.8 Hz above baseline, sign test: p = 0.71; Fig. 13 A) and the cumulative histogram of response amplitudes showed little or no change (Fig. 13 B). The analysis of individual responses, however, revealed that AP5 increased some responses and decreased others. Consequently, the distribution of responses across the population of MCs in the presence of AP5 was different from control (Fig. 13 C). PSTHs revealed that the average time course of MC firing was similar to control (Fig. 13 D) but individual MC responses could be increased or decreased, often within certain time windows (Fig. 13 E). Largest changes were observed shortly after response onset, but later phases could also be affected. Hence, AP5 had little effect on the average magnitude and time course of the population response but caused complex changes of individual MC responses and spatio-temporal activity patterns.

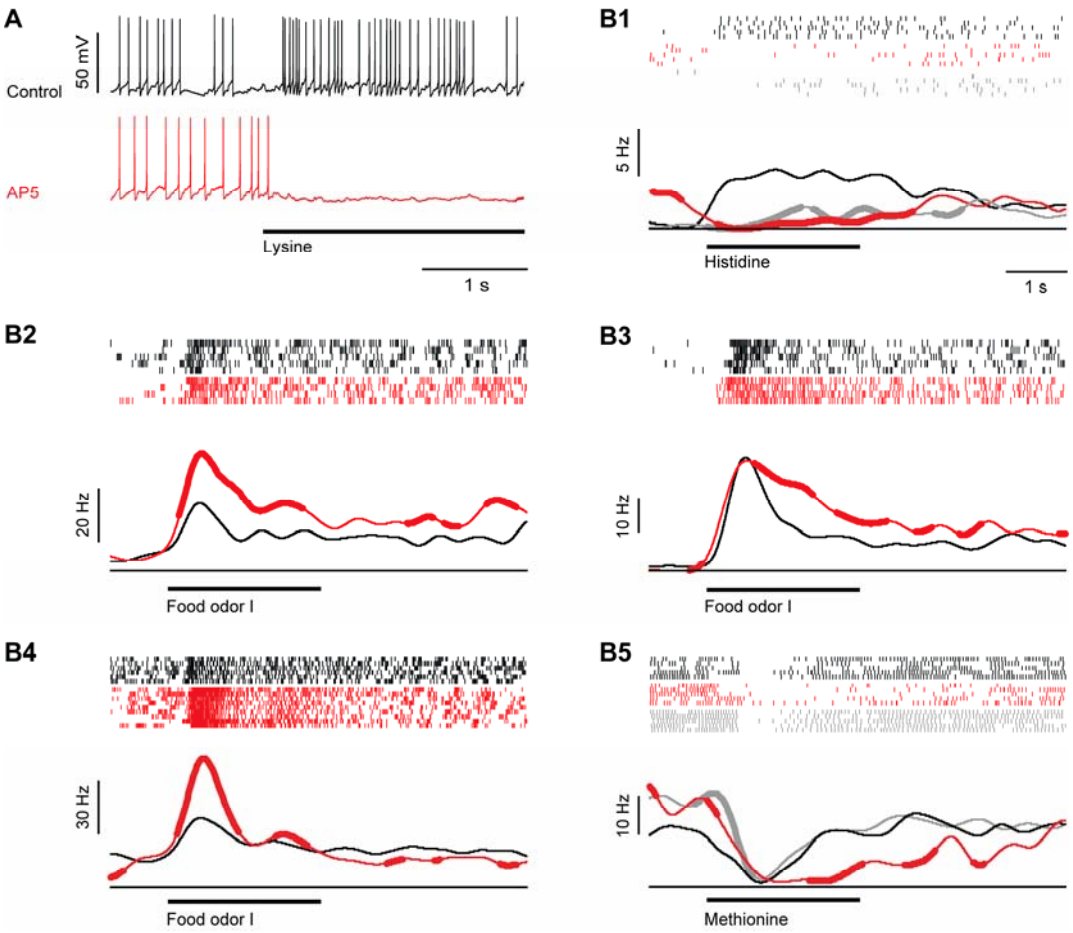

Figure 12. Effect of the NMDAR antagonist, AP5, on odor responses of MCs. (A) Whole-cell recording of a MC response to odor stimulation (Lys, 10 µM; bar) before (black) and during (red) application of AP5. (B1 – B5) Five examples illustrating effects of AP5 on odor responses. Conventions as in Fig. 3. Responses are from different cells and were recorded in the whole-cell, cell-attached or loose-patch configuration. (Tabor and Friedrich, 2008)

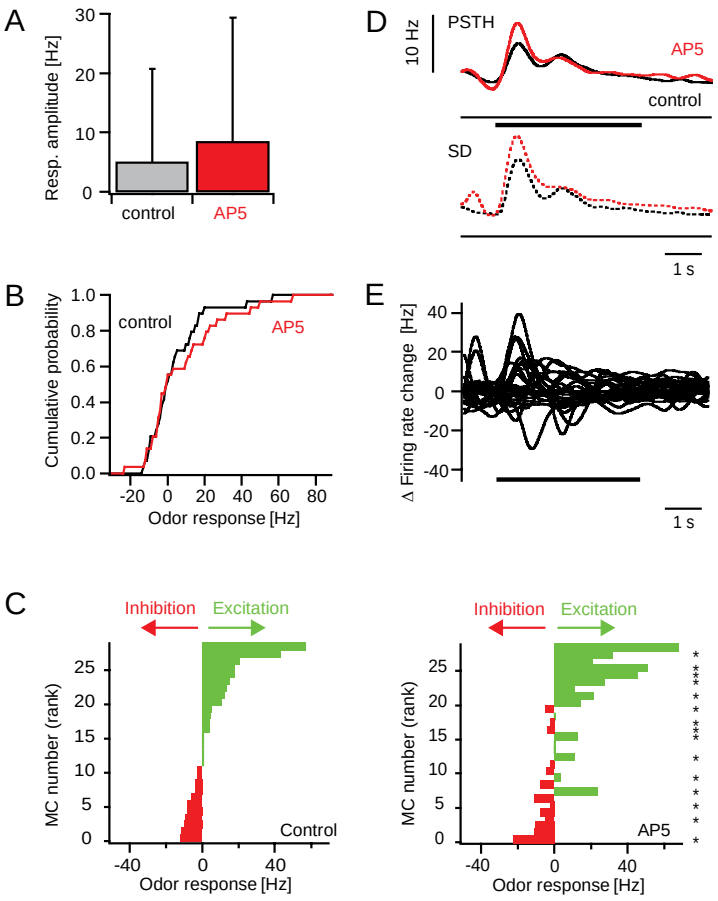

Figure 13. Effect of AP5 on odor responses of MCs: quantitative analysis. (A) Mean firing rate change evoked by odor stimulation before (control) and during AP5 treatment in the time window between 0.25 and 0.75 s after response onset. (B) Cumulative distribution of odor-evoked firing rate changes in MC before (control) and during application of AP5. (C) Left: MC odor responses ranked according to the firing rate change measured before application of AP5. Right: Responses of the same MCs to the same odors in the presence of AP5 (same rank order as control). Asterisks denote responses that were significantly changed in the presence of AP5 (t-test; $P < 0.05$). (D) Top (continuous lines): average PSTH of MC odor responses before (control) and during application of AP5. Thick portions depict time bins where the PSTH in the presence of AP5 was significantly different from the control PSTH in the corresponding time bin (sign test; $P < 0.05$). Bottom (dashed lines): SD. (E) Differences of PSTHs (AP5 – control) for all MC odor responses. (Tabor and Friedrich, 2008)

Effects of ionotropic glutamate receptor antagonists on local field potential oscillations

In the absence of drugs, all stimuli evoked LFP oscillations with a frequency of around 20 Hz (Fig. 14 A, B). Because amplitudes were largest in response to food extracts, I concentrated on these stimuli for further experiments. NBQX completely abolished LFP oscillations in response to food odors (n = 6 OBs; 5 ± 1 % of control power in 15 – 30 Hz band; t-test: $P < 0.001$; Fig. 14 A, C). AP5 reduced, but not completely abolished, LFP oscillations (4 OBs; 44 ± 30 % of control power in 15 – 30 Hz band; t-test: $P < 0.01$; Fig. 14 B, C). Moreover, the oscillation frequency was slightly increased compared to control in all experiments (Fig. 14 B). The effects of both drugs were reversible after washout.

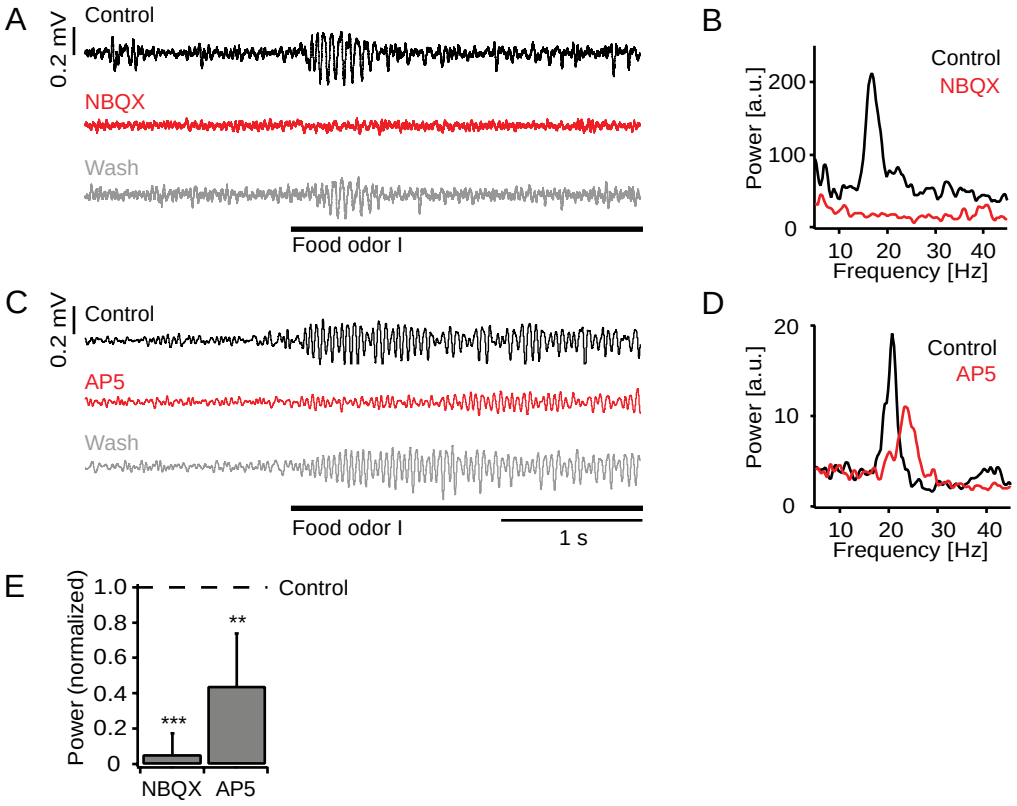

Figure 14. Effect of NBQX and AP5 on LFP oscillations. (A) Example of an LFP recording (bandpass-filtered 8 – 43 Hz) of an odor response (food odor; bar) before (black), during (red) and after (gray) application of NBQX. (B) Power spectra of LFP responses before and during application of NBQX (same recording; average of 7 trials; calculated from raw data). (C) and (D) Effect of AP5 on LFP oscillations evoked by food odor stimulation. (conventions as in (A) and (B) Power spectra are average of 14 trials). (E) Average LFP power (15 – 30 Hz) in the presence of NBQX (n = 6 OBs) or AP5 (n = 4 OBs), normalized to control. ***, $P < 0.001$; **, $P < 0.01$ (t-test). (Tabor and Friedrich, 2008)

Measurements of odor-evoked activity patterns by two-photon Ca^{2+}-imaging

Although AMPA receptors and NMDA receptors mediate excitatory synaptic input from OSNs to MCs, the blockade of one receptor type alone did not reduce the average excitation of MCs, suggesting that iGluRs also influence MC responses via other, multisynaptic pathways. I therefore analyzed the effect of iGluR antagonists on network activity patterns using two-photon Ca^{2+}-imaging after bolus loading of OB neurons with the red-fluorescent Ca^{2+}-indicator, rhod-2. MCs and INs were distinguished by the expression of the MC marker, HuC:YC, that was detected simultaneously in a separate emission channel. Somatic Ca^{2+}-signals reflect the spike output of individual MCs and INs (Yaksi and Friedrich, 2006) and are stable over hours (Yaksi et al., 2007). Two-photon Ca^{2+}-imaging therefore permits measurements of odor-evoked action potential firing from many neurons, including INs in deep layers that are difficult to record using electrophysiological methods.

I first examined the effect of glutamate receptor antagonists on odor-evoked Ca^{2+}-signals of MCs before, during and after drug treatment using the same protocol as before (Fig. 15 A). In many MCs, NBQX increased the amplitude of odor-evoked Ca^{2+}-signals, while decreases in response amplitude were rarely observed. On average, NBQX significantly increased Ca^{2+}-signals (150 % of control; sign test: $P = 0.002$; Fig. 15 B). Consequently, the cumulative distribution of response amplitudes was shifted towards higher amplitudes (Fig. 15 C). At the level of individual MCs, the effect of NBQX varied in magnitude (Fig. 15 D, E). The correlation coefficient between MC activity patterns before and during NBQX treatment was 0.73 (Fig. 15 D; $n = 190$ responses, pooled over all MCs and odors). As a control, I performed the same procedures in a different set of fish except that NBQX was omitted during the wash-in period. The correlation between activity patterns in these control experiments ($r = 0.78$; $n = 126$ responses) was slightly, but not significantly ($P = 0.32$), higher than in experiments using NBQX. Hence, NBQX increased the amplitude of the MC population response but had little or no effect on the odor-evoked pattern of Ca^{2+} signals across the MC population.

Blockade of NMDA receptors by AP5 had diverse effects on odor-evoked Ca^{2+} signals of individual MCs, including increases and decreases of the response (Fig. 16 A). The average response amplitude was not significantly different from control (86 % of control; $p = 0.26$; sign test; Fig. 16 B) and the cumulative histogram of response amplitudes showed no obvious change (Fig. 16 C). However, the activity pattern across the MC population differed from control because some responses were increased while others were decreased (Fig. 16 D, E).

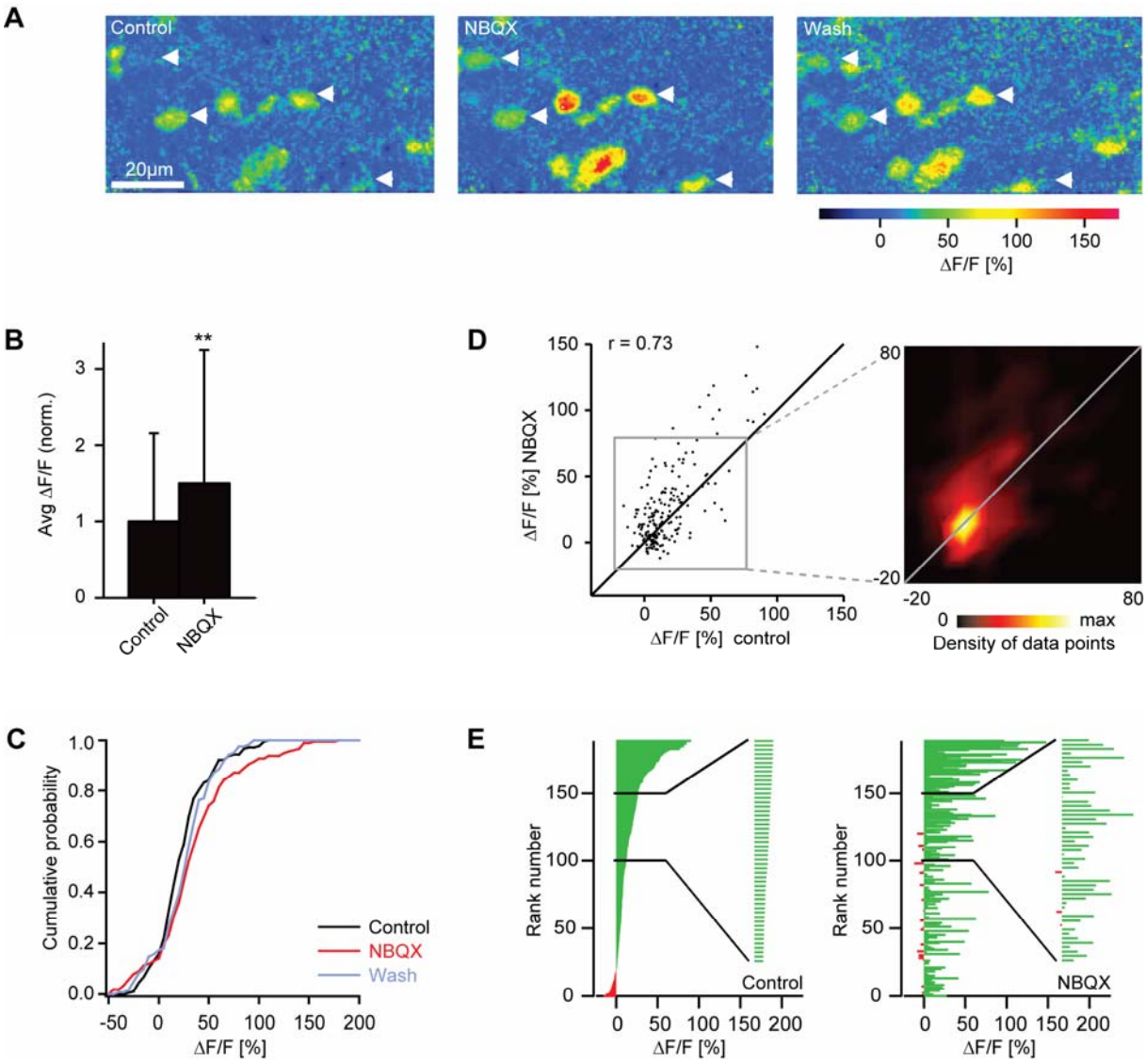

Figure 15. Effect of NBQX on MC responses measured by two-photon Ca^{2+}-imaging. (A) Odor-evoked Ca^{2+}-signals in MCs before, during and after application of NBQX (stimulus: Trp, 10 µM). Arrows depict somata of neurons identified as MCs by expression of the genetically encoded fluorescence marker HuC-YC. (B) Average somatic Ca^{2+}-signals before (control) and during application of NBQX, normalized to control. Error bars show SD. **, P = 0.002 (sign test). (C) Cumulative distribution of Ca^{2+}-signal amplitudes before (black), during (red) and after (gray) application of NBQX. (D) Comparison of Ca^{2+}-signal amplitudes evoked by the same odors in the same MCs before and during application of NBQX. Data were pooled over all cells, odors and animals (n = 190 responses). r, Pearson correlation coefficient. Inset shows the density of data points in the boxed region. Lines are diagonals with slope one. (E) Left: MC odor responses ranked according to the Ca^{2+}-signal before application of NBQX. Inset shows an enlargement of a subregion. Right: Responses of the same MCs to the same odors in the presence of NBQX, ranked in the same order as in the control. (Tabor and Friedrich, 2008)

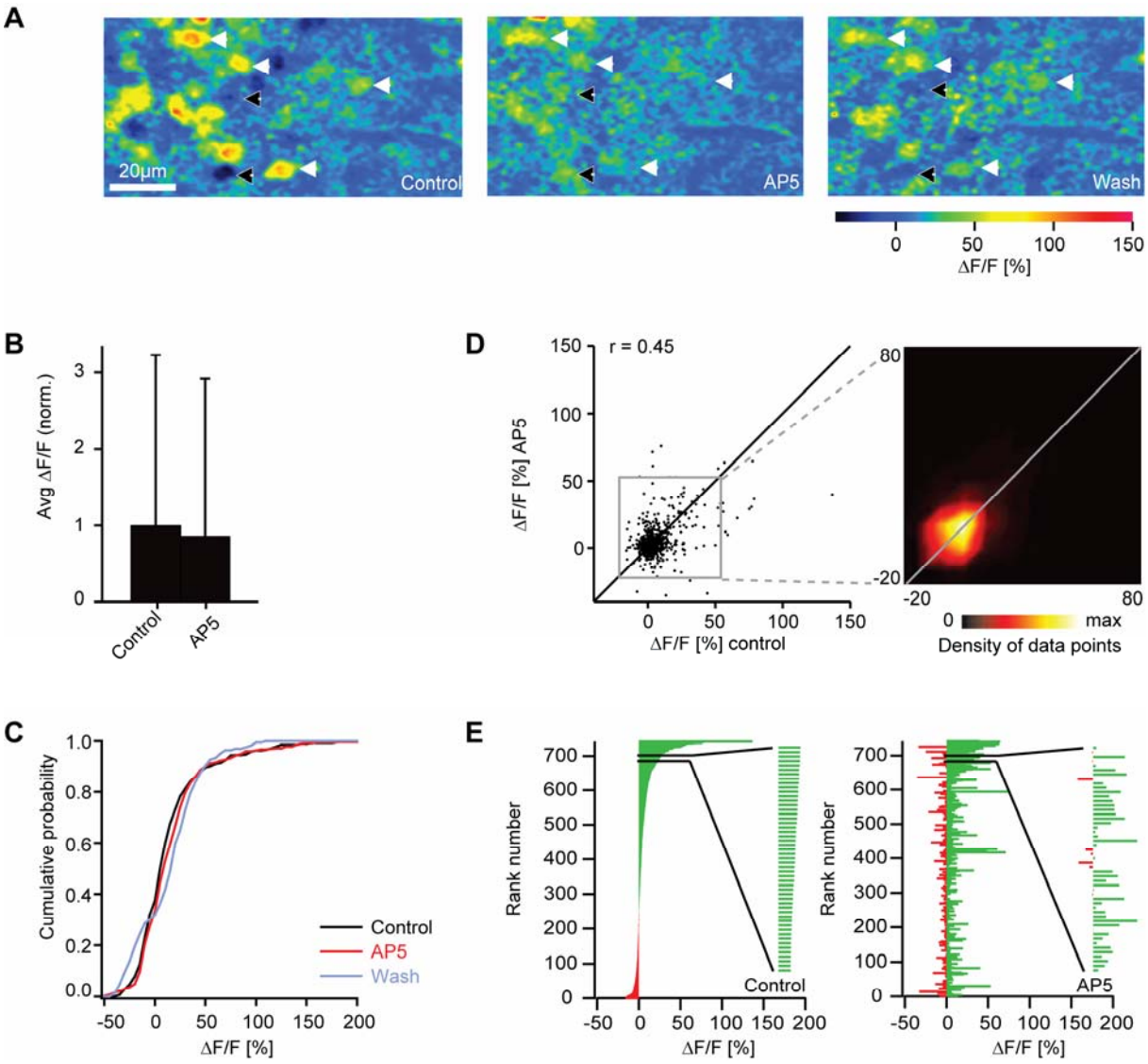

Figure 16. Effect of AP5 on MC responses measured by two-photon Ca^{2+}-imaging. (A) Odor-evoked Ca^{2+}-signals in MCs before, during and after application of AP5 (stimulus: food odor). Arrows depict somata of neurons identified as MCs by expression of the genetically encoded fluorescence marker HuC-YC. Black and white arrows show MCs whose response was increased and decreased, respectively, by AP5 treatment. (B) Average somatic Ca^{2+}-signals before (control) and during application of AP5, normalized to control. Error bars show SD. (C) Cumulative distribution of Ca^{2+} signal amplitudes before (black), during (red) and after (gray) application of AP5. (D) Comparison of Ca^{2+}-signal amplitudes evoked by the same odors in the same MCs before and during application of AP5. Data were pooled over all cells, odors and anminals (n = 742 responses). r, Pearson correlation coefficient. Inset shows the density of data points in the boxed region. Lines are diagonals with slope one. (E) Left: MC odor responses ranked according to the Ca^{2+}-signal before application of AP5. Inset shows an enlargement of a subregion. Right: Responses of the same MCs to the same odors in the presence of AP5, ranked in the same order as in the control. (Tabor and Friedrich, 2008)

The correlation between activity patterns before and during AP5 treatment was 0.45 (n = 742 responses) and significantly different from control (r = 0.78; n = 126 responses; $P < 0.001$). Hence, AP5 did not significantly affect the mean response amplitude of MCs but changed the pattern of activity across the population. The effects of AP5 and NBQX on odor-evoked patterns of Ca^{2+}-signals across MCs are therefore consistent with those observed by electrophysiological measurements.

Effects of ionotropic glutamate receptor antagonists on interneuron activity

Somata of INs in the deeper layers of the OB are densely packed and show pronounced Ca^{2+}-signals in response to odor stimulation (Fig. 10A; Yaksi and Friedrich, 2006; Yaksi et al., 2007). In the presence of NBQX, response amplitudes of many INs were decreased and response patterns appeared sparser. Ca^{2+}-signals in the neuropil were also substantially reduced (Fig. 10A). The average somatic Ca^{2+}-signal of INs was significantly smaller than control (47 % of control; sign test: $P < 0.001$; Fig. 10B) and the cumulative distribution of response amplitudes was shifted towards lower amplitudes (Fig. 10C). NBQX therefore increased the ratio between the mean MC response and the mean IN response by a factor of 3.2. At the level of individual IN somata, the effect of NBQX was diverse. Not all responses were reduced by the same amount, and some responses were even enhanced (Fig. 10A, D, E). The correlation between activity patterns before and during NBQX treatment was 0.41 (n = 5878 responses; pooled over all INs and odors) and significantly lower than the correlation between activity patterns in control experiments without drugs (r = 0.71; n = 208 responses; $P < 0.001$). Hence, blockade of AMPA receptors decreased the mean response of INs and changed the activity pattern across the IN population.

Blockade of NMDA receptors by AP5 caused only a slight change in the mean response amplitude of INs (109 % of control; sign test: $P < 0.001$; Fig. 11A, B) and the cumulative histogram of response amplitudes remained similar (Fig. 11C). AP5 therefore changed the ratio between the mean MC response and the mean IN response by a factor of 0.79. Individual IN responses, however, were often increased or decreased by AP5 (Fig. 11D, E). The correlation between activity patterns before and during AP5 treatment was 0.40 (n = 14884 responses) and significantly different from control (r = 0.71; n = 208 responses; $P < 0.001$). Hence, the blockade of NMDA receptors had little effect on the overall amplitude of IN responses but caused a redistribution of activity across the population.

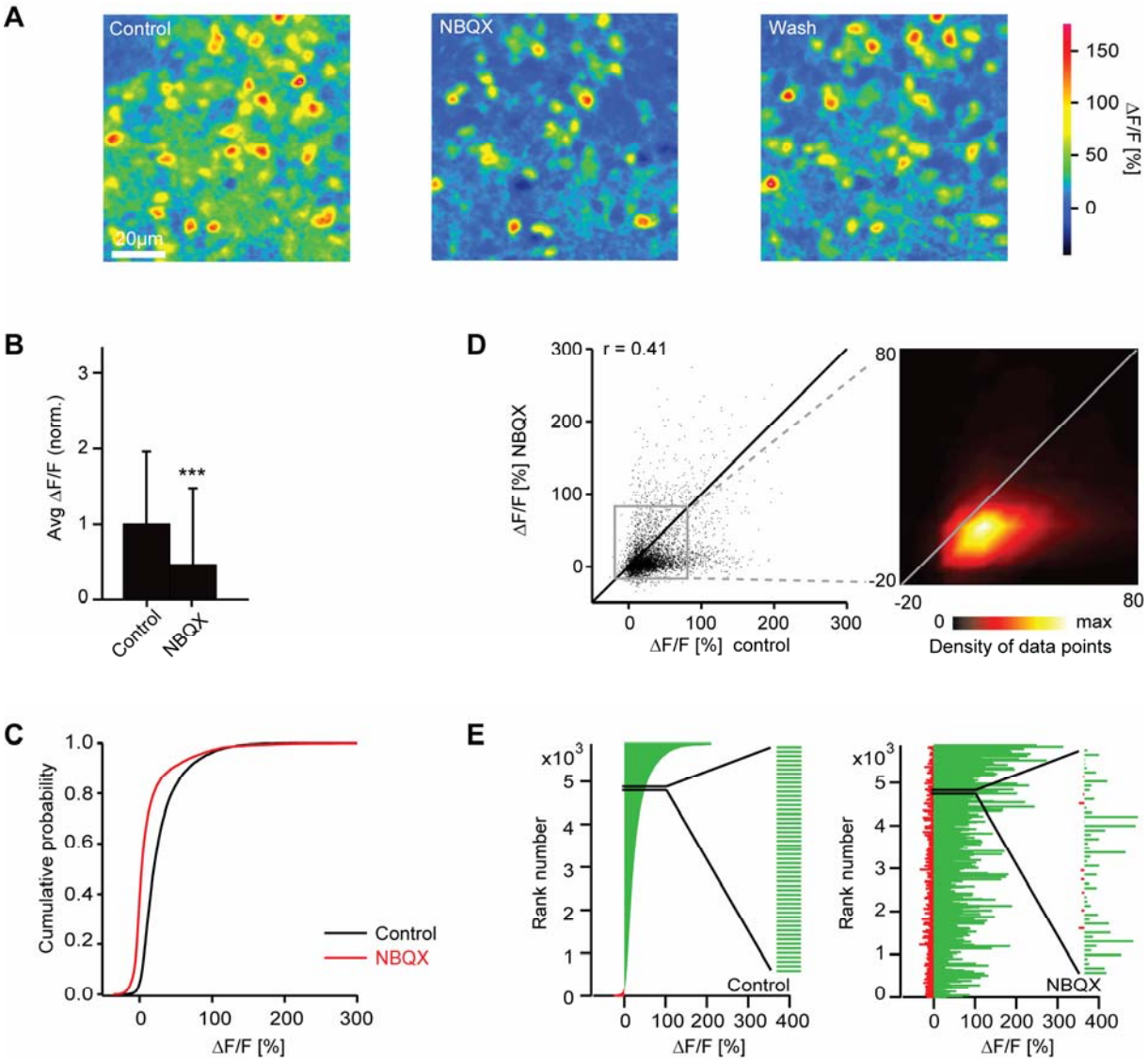

Figure 17. Effect of NBQX on IN responses measured by two-photon Ca^{2+}-imaging. (A) Odor-evoked Ca^{2+}-signals in INs before, during and after application of NBQX (stimulus: food odor). (B) Average somatic Ca^{2+}-signals before (control) and during application of NBQX, normalized to control. Error bars show SD. ***, $P < 0.001$ (sign test). (C) Cumulative distribution of Ca^{2+}-signal amplitudes before (black) and during (red) application of NBQX. (D) Comparison of Ca^{2+}-signal amplitudes evoked by the same odors in the same INs before and during application of NBQX. Data were pooled over all cells, odors and anminals (n = 5878 responses). r, Pearson correlation coefficient. Inset shows the density of data points in the boxed region. Lines are diagonals with slope one. (E) Left: IN odor responses ranked according to the Ca^{2+}-signal before application of NBQX. Inset shows an enlargement of the boxed region. Right: Responses of the same INs to the same odors in the presence of NBQX, ranked in the same order as in the control. Inset shows an enlargement of a subregion to demonstrate that low-amplitude values are interspersed between high amplitude values. The visual impression in the full diagram that many amplitudes are increased during NBQX treatment is therefore an artifact caused by crowding of bars in the graph. (Tabor and Friedrich, 2008)

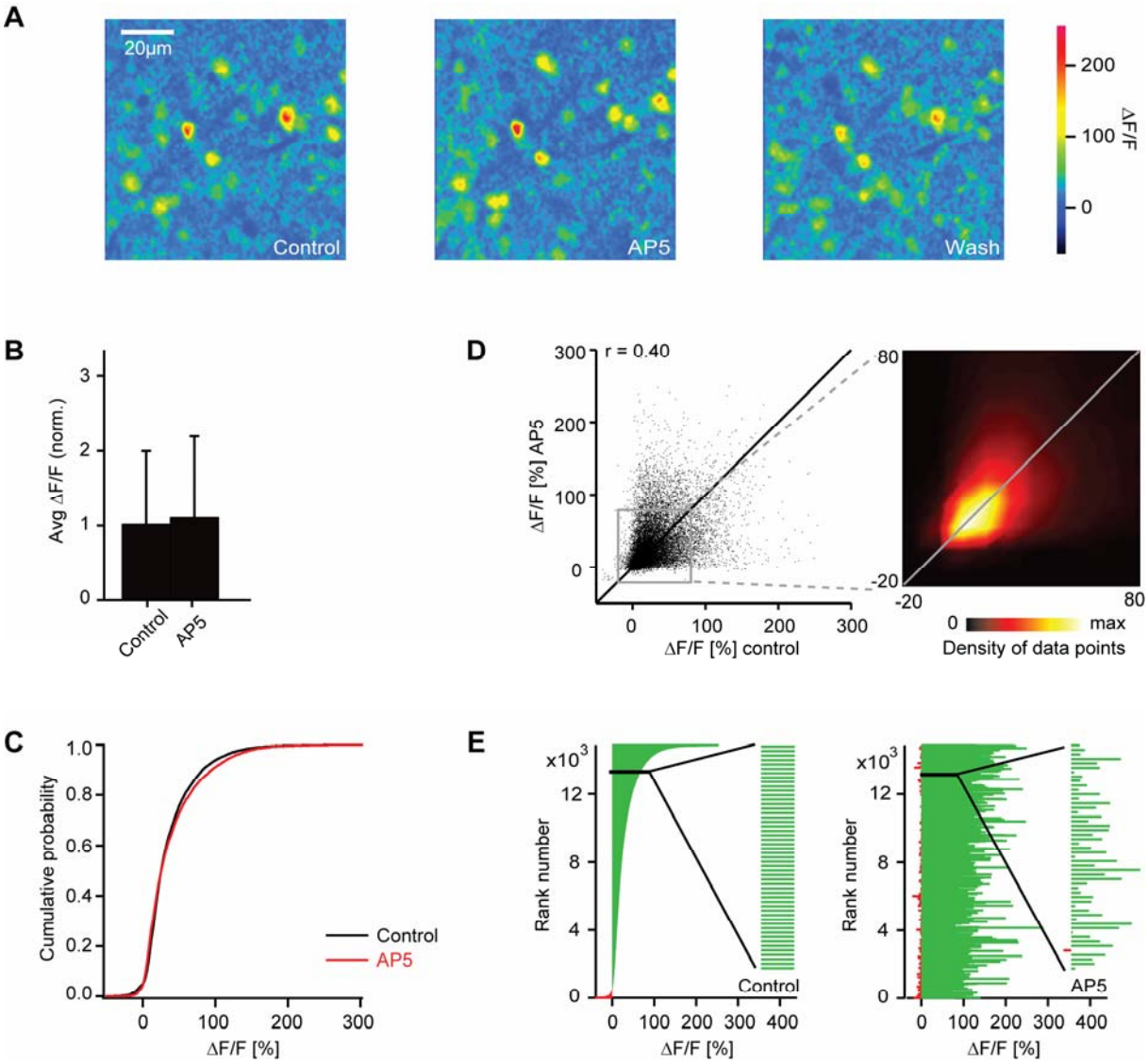

Figure 18. Effect of AP5 on IN responses measured by two-photon Ca^{2+}-imaging. (A) Odor-evoked Ca^{2+} signals in INs before, during and after application of AP5 (stimulus: food odor). (B) Average somatic Ca^{2+}-signals before (control) and during application of AP5, normalized to control. Error bars show SD. ***, $P < 0.001$ (sign test). (C) Cumulative distribution of Ca^{2+}-signal amplitudes before (black) and during (red) application of AP5. (D) Comparison of Ca^{2+} signal amplitudes evoked by the same odors in the same INs before and during application of AP5. r, Pearson correlation coefficient. Inset shows the density of data points in the boxed region. Lines are diagonals with slope one. (E) Left: IN odor responses ranked according to the Ca^{2+}-signal before application of AP5. Data were pooled over all cells, odors and anminals (n = 14884 responses). Inset shows an enlargement of the boxed region. Right: Responses of the same INs to the same odors in the presence of AP5, ranked in the same order as in the control. Inset shows an enlargement of a subregion to demonstrate that low-amplitude values are interspersed between high amplitude values. The visual impression in the full diagram that many amplitudes are increased during AP5 treatment is therefore an artifact caused by crowding of bars in the graph. (Tabor and Friedrich, 2008)

Discussion

I used pharmacological manipulations in combination with electrophysiology and Ca^{2+}-sensitive fluorescence imaging to study the functions of GABA receptors and iGlu receptors in neuronal circuits of the intact OB. Electrophysiological recordings monitor action potentials and subthreshold synaptic input at high temporal resolution and were used to analyse spontaneous and odor evoked MC activity. Ca^{2+}-sensitive fluorescence measurements allow observations of spatially distributed activity patterns. Terminals from OSNs were imaged with a Camera system while two-photon imaging was used to measure odor responses of INs and in some cases of MCs with single cell resolution. Both recording methods have complementary advantages and yielded consistent results. The blockade of GABA(B) receptors increased odor evoked Ca^{2+}-signals in the terminals of OSNs and modulated responses in a subset of MCs. The blockade of GABA(A) receptors amplified spontaneous and odor evoked MC activity, induced burst firing, abolished odor evoked oscillations in the LFP and changed the slow temporal modulations of MC odor responses. The combined blockade of AMPA receptors and NMDA receptors completely suppressed spontaneous and odor-evoked activity of MCs. The selective blockade of AMPA receptors or NMDA receptors, however, did not decrease the mean response of MCs but had complex effects on neuronal responses. AMPA receptor blockade rather increased MC responses and particularly NMDA receptor blockade changed the spatio-temporal patterns of activity across MC and IN populations. The results indicate that the studied receptors fulfil differential functions during odor processing and provide insights into mechanisms for slow temporal modulations of MC responses, synchronization of neurons and gain control.

Functions of presynaptic inhibition of sensory input by GABA(B) receptors

Studies in the rat showed, that GABA(B) receptors are densely expressed in the glomerular layer while their expression in other layers is much lower (Bowery et al., 1987; Chu et al., 1990; Panzanelli et al., 2004) This suggests a predominant role of GABA(B) receptors for presynaptic inhibition of the sensory input. Therefore, I examined the impact of GABA(B) receptors on Ca^{2+}-signals in terminals of zebrafish OSNs. I found that odor evoked Ca^{2+}-signals were increased by the specific GABA(B) receptor antagonist CGP54626 while they were reduced by the specific agonist baclofen. This is consistent to observations in other

species including vertebrates and invertebrates (Wachowiak and Cohen, 1999b; McGann et al., 2005; Wachowiak et al., 2005b; Vucinic et al., 2006). The presynaptic modulation of sensory input by GABA(B) receptors appears therefore to be a common principle in the olfactory system.

The function of GABA(B) receptors on the axon terminals of OSNs might be to mediate presynaptic gain control or to participate in the modulation of spatio-temporal activity patterns. Experiments in mice indicated that a reduction of the presynaptic Ca^{2+}-signal mediated by GABA(B) receptors is accompanied by even stronger reduction in transmitter release (Wachowiak et al., 2005b) which might be caused by a Ca^{2+}-independent second messenger pathway that modulates priming of synaptic vesicles (Sakaba and Neher, 2003). This suggests a substantial influence on the gain of glomerular input and might lead to a pronounced effect on postsynaptic excitation. This mechanism might be involved in the adjustment to changing stimulus conditions. Other Ca^{2+}-imaging studies indicated that glomeruli might be modulated independently by self-inhibition (McGann et al., 2005; Wachowiak et al., 2005b; Vucinic et al., 2006). As glomerular activity patterns evoked by similar odors often overlap primarily in clusters of strongly responsive units, this mechanism could reduce the relative contribution of such units to the whole activity pattern, thereby contributing to fine discrimination. Further, presynaptic inhibition may affect the temporal patterning of glomerular input signals (Spors et al., 2006) and MC responses and thereby also influence odor processing.

In my experiments spontaneous activity was unchanged when GABA(B) receptors were blocked. This result is consistent with previous findings in the frog (Duchamp-Viret et al., 2000). In contrast to that, the activation of GABA(B) receptors was shown to reduce or even completely block spontaneous activity in MCs (Duchamp-Viret et al., 2000; Palouzier-Paulignan et al., 2002). Different specific antagonists can restore spontaneous MC activity from GABA(B) receptors mediated inhibition but do not elicit a further increase. Together this suggests that GABA(B) receptors are not activated during spontaneous activity. It is likely that synaptic activity needs to exceed a certain threshold before interneurons release sufficient amounts of GABA for the paracrine activation of presynaptic receptors.

MC responses evoked by odor stimulation (Duchamp-Viret et al., 2000) or brief electrical pulses (Nickell et al., 1994; Aroniadou-Anderjaska et al., 2000; Palouzier-Paulignan et al., 2002) are usually reduced by GABA(B) receptor-mediated inhibiton. The blockade of GABA(B) receptors in the experiments here in contrast changed response amplitude only in a subset of MCs without major effect on the average activity. Similarly experiments in the

intact frog brain failed to demonstrate an effect of the GABA(B) receptor antagonist on odor-evoked activity (Duchamp-Viret et al., 2000). This is somewhat surprising, as the presynaptic Ca^{2+}-responses evoked by odor stimulation were clearly increased.

The data presented here show a prominent role of inhibitory feedback from local circuits in the OB for the regulation of MC excitability. The mean MC response amplitude in my experiments at least had a slight tendency to be amplified during blockade of GABA(B) receptors, although not statistically significant. A stronger inhibitory feedback from local interneurons might therefore cover the effect of amplified sensory input. A study of glomerular response patterns induced by GABA(B) receptor blockade indicated that strongly activated glomeruli inhibit the surrounding ones (Vucinic et al., 2006). Glomeruli inside centres of high activity might therefore benefit more from a GABA(B) receptor blockade than moderately activated glomeruli further apart. Further, as synaptic activity apparently needs to exceed a certain threshold for GABA(B) receptor activation, autoinhibition of glomerular activity might be inactive in weaker activated glomeruli. The antagonist then affected only a small subset of glomeruli while many glomeruli are not affected. This may also explain the high variability of effects observed across odor responses in MCs. MC excitation, therefore, appears under control of inhibitory interneurons and not linerarly dependent on presynaptic input signal. Experiments in the rat revealed further, that GABA release from interneurons can be inhibited through GABA(B) receptors (Isaacson and Vitten, 2003). It appears possible that the amplified sensory input here is partially compensated by increased GABA(A) mediated feedback from disinhibited INs. The results indicate that network circuits largely compensate for changes in total afferent excitation.

The slow kinetic of this metabotropic receptor suggests a role for periods of inhibition during MC odor responses lasting from tens to thousands of milliseconds. The data presented here show that GABA(B) receptor blockade changed odor-evoked response patterns in MCs in early and late phases of the response. On average the effect did not decline during the time course of MC odor responses while GABA(A) receptors blockade primarily amplified a transient phase immediately after odor response onset. Similar results were reported from experiments on the output neurons in the antennal lobe of Drosophila (Wilson and Laurent, 2005). GABA(B) receptor mediated influences on MC response are therefore distinct from those of GABA(A) receptors. GABA(B) receptors appear to participate in the generation of long-lasting phases of inhibition in MC responses but do not provide the only mechanism, as such inhibitory epochs were still observed and sometimes even enhanced in the presence of the GABA(B) receptor antagonist. Beyond the presynaptic inhibition of afferents GABA(B)

receptors were also found to modulate GABA release from INs, already mentioned above. Although functional evidence for a direct inhibition of MCs is still missing, GABA(B) receptor expression in the MC layer was found, too (Bonino et al., 1999; Margeta-Mitrovic et al., 1999). The slow modulations of the MC response might therefore involve receptors at multiple levels in the OB network.

Receptors involved in the regulation of neuronal excitability

The sensory input to the OB network varies substantially in strength and complexity depending on concentration and composition of the odor stimulus. Transmission of the sensory signal to MCs and inhibitory input from OB interneurons, both shape the output signal. The regulation of neuronal excitability is central to the adaptation to changing stimulus conditions.

Here, I found that a combined blockade of AMPA receptors and NMDA receptors completely suppressed spontaneous and odor-evoked activity of MCs. This indicates that excitatory synaptic transmission from OSNs to MCs is mainly mediate by iGlu receptors, as reported in other vertebrates (Berkowicz et al., 1994; Ennis et al., 1996). Paradoxically, however, the selective blockade of AMPA receptors or NMDA receptors did not decrease the mean response of MCs. Rather, the AMPA receptor antagonist even increased the mean MC response, and both antagonists had complex effects on neuronal responses including changes in the sign. These effects cannot be explained by a partial blockade of the excitatory OSN→MC synapse alone, but imply that iGlu receptors influence MC firing also via additional, multisynaptic pathways. The increased excitability must be based on a strong reduction of inhibitory feedback from local INs. The most obvious pathways are the OSN→juxtaglomerular cell→MC and the MC→IN→MC pathway. The results therefore indicate that OB output activity is strongly influenced by synaptic pathways within and possibly beyond the OB.

AMPA and NMDA receptors not only mediate excitatory transmission from OSNs to MCs but are also involved in synaptic pathways that activate inhibitory INs. The net effect of an iGlu receptor antagonist on mean MC response amplitudes may therefore be reduced, unchanged, or even increased responses, depending on the relative contribution of each iGlu receptor type to each of these pathways. Although NBQX partially blocks excitatory synaptic transmission from OSNs to MCs, it increased the mean response of MCs. This indicates that AMPA receptor blockade strongly attenuates input from inhibitory INs. Consistently I found

the mean response of INs significantly decreased. This hypothesis is further supported by experiments performed in brain slices of the rat, where AMPA receptors appeared important for the activation of GABAergic interneurons (Schoppa, 2006b). The ratio between excitation and inhibition of MCs therefore depends on circuits with multisynaptic AMPA receptor signaling. Pathways as the OSN→juxtaglomerular cell→MC pathway, the MC→IN→MC pathway or glutamatergic connections from higher brain areas terminating on INs are likely involved. Hence, the GABAergic inhibitory system is closely linked to AMPA receptor signaling, which is thereby involved in the regulation of MC population activity during an odor response.

The occurrence of prominent odor responses in the presence of NBQX confirms that NMDA receptors contribute to basal synaptic transmission in the OB (Trombley and Westbrook, 1990; Aroniadou-Anderjaska et al., 1999b; Edwards and Michel, 2002) under natural conditions. Unlike the blockade of AMPA receptors, however, the blockade of NMDA receptors had little or no effect on the mean activity of MCs and INs. Nevertheless, I observed changes in the magnitude and time course of individual MC responses. NMDA receptors therefore appear less important for the global regulation of MC population activity than AMPA receptors.

Inhibitory input to MCs is provided from GABAergic INs in the OB and mediated by activation of GABA(A) receptors (Nowycky et al., 1981; Wellis and Kauer, 1993; Lowe, 2002). However, the effect of GABA(A) receptor antagonists on odor responses in the intact olfactory system has been examined only in insects, so far (MacLeod and Laurent, 1996; Wilson and Laurent, 2005). Here I found that blockade of GABA(A) receptors enhanced spontaneous activity and odor-evoked excitation of MCs in the intact olfactory bulb of zebrafish. The results indicate, that GABA(A) receptors are crucial for the regulation of the OB output.

The increased spontaneous firing rates indicate that MCs in an intact olfactory system are under tonic inhibition from local INs. Spontaneous subthreshold fluctuations are likely to be of synaptic origin and suggest continuous excitatory and inhibitory input from primary afferents and local INs. A result that is expected as MCs in the intact OB are spontaneously active (MacLeod, 1976; Kay and Laurent, 1999; Friedrich and Laurent, 2001).

Gabazine particularly amplified firing rates during the initial phase of an odor response similar to NBQX. Hence, the pharmacological manipulation of GABA(A) receptors and AMPA receptors apparently changes the ratio between excitatory and inhibitory input to MCs. This indicates that inhibitory GABAergic feedback onto the population of MCs strongly

influences MC firing and performs a gain control at the population level that regulates MC firing when the intensity of glomerular inputs varies. Indeed, the total firing of MCs converges towards a common level within a few hundred milliseconds in response to odors that evoke different amounts of sensory input (Friedrich and Laurent, 2004).

The blockade of GABA(A) receptors, furthermore, led to rhythmical burst in subsets of MCs before and most MCs after stimulus onset. The exact frequency was variable among odor responses and might even change during the odor response. However, a broad but clear peak in the averaged power spectral density graph marked 1Hz as mean frequency. This was at least similar to the frequency observed under the same conditions in the LFP but without stimulation. This might indicate that the network changed into a different physiological state of massively synchronized and rhythmical activty. The lack of inhibition may enable spontaneous excitatory events to drive the MC membrane potential above firing threshold. Hyperpolarizations which terminate phases of raised activity might be caused by intrinsic, activity dependent conductances, as Ca^{2+}-activated K^{+}-channels (Knaus et al., 1996) and/or synaptic input.

Blockade of GABA(A) receptors is known to induce epileptiform activity in other brain areas, such as cortex, hippocampus and thalamus (for review see: Traub et al., 1996; McCormick and Contreras, 2001). The rhythm of such persistent bursting is thought to depend on neurons able to generate bursts intrinsically and rhythmic interplay between excitatory and inhibitory neurons. Mechanisms leading to prolonged depolarizations which underlie intrinsic bursts can be persistent voltage gated sodium currents or slow dendritic Ca^{2+}-spikes (Azouz et al., 1996). In synapses NMDA receptors can evoke long-lasting depolarizations. Voltage-, Ca^{2+}- or Na^{+}-activated K^{+}-currents seem to determine the hyperpolarization period after the burst intrinsically. But also synaptic inhibition as in thalamo-cortical interactions through GABA(B) receptors can be involved. It appears likely, that mechanisms involved in the generation of epileptiform activity, are also responsible for the rhythmic bursting observed here.

Epileptic activity usually depends on recurrent excitatory connections. Long-lasting depolarizations in MCs leading to rhythmical bursting with about 1 Hz were described in rat slices (Carlson et al., 2000; Puopolo and Belluzzi, 2001) and appeared based on intraglomerular dendrodendritic interactions. MCs associated with the same glomerulus can excite one another by gap junctions and spillover of dendritically released glutamate (Carlson et al., 2000; Urban and Sakmann, 2002; Christie and Westbrook, 2006). During blockade of

GABA(A) mediated inhibitory network feedback, intraglomerular recurrent excitatory mechanisms might be involved in the synchronization of MC activity.

The generation of bursts demands mechanisms that mediate prolonged periods of excitation. Massive release of glutamate upon strong neuronal activity is likely to facilitate spillover. This might activate NMDA receptors, which may even prolong excitation periods in MCs by autoexcitation (Aroniadou-Anderjaska et al., 1999a; Isaacson, 1999b; Friedman and Strowbridge, 2000; Didier et al., 2001; Salin et al., 2001). Experiments on slices of rat OBs revealed, that the blockade of NMDA receptors prevents rhythmical burst generation (Puopolo and Belluzzi, 2001). Moreover, a subclass of juxtaglomerular neurons in rodents, the external tufted cells, were shown to intrinsically generate burst with help of a persistent voltage activated Na^+-conductance (Hayar et al., 2004). A similar type of neurons might also exist in zebrafish. Both mechanisms might be involved and lead to burst firing in MCs.

Inter-burst intervals usually lack action potential firing and suggest that mechanisms are involved, which mediate long-lasting inhibition or prevent firing intrinsically. Gabazine-insensitive inhibitory synaptic input might be provided by the activation of GABA(B) receptors. Their expression on MC dendrites was shown in mice (Kratskin et al., 2006). But also glycinergic synaptic transmission might be involved that has been shown to inhibit MCs in the rat OB (Trombley and Shepherd, 1994; Trombley et al., 1999). In situ hybridization experiments in zebrafish found glycine receptor subunits only in the internal cellular layer, which might indicate that only INs receive glycinergic input (Imboden et al., 2001). However, functional studies are still missing. Also a remaining effect of GABA can not be ruled out, as Gabazine is an competitive inhibitor of GABA(A) receptors which shifts the concentration-response curve to higher GABA concentrations without changing the maximal response (Hamann et al., 1988). In addition, MCs might be inhibited by Ca^{2+}-activated K^+-currents (Knaus et al., 1996). MCs often showed a prolonged period of hyperpolarization after intense firing, which might indicate that a Ca^{2+}-activated K^+-current is involved. However, in some cases hyperpolarizations without preceding firing was observed, too. Hence, this suggests that both intrinsic and synaptic effects play a role.

Further, also ephaptic effects might contribute to the generation of epileptiform activity. Massively synchronized bursting in epileptic brain centers can cause strong, pulsating electrical fields which might contribute to coupling of neurons. Such intensive neuronal activity might even cause changes of extracellular ion- concentrations. A reduced K^+-gradient for example can depolarize neurons and thereby facilitate action potential

generation. Here, ephaptic effects based on changes of extracellular K^+- or Ca^{2+}-concentrations are unlikely in the OB because the bath solution was continuously exchanged but might play a role inside brain structures still covered by bones and skin. In the experiments discussed here the GABA(A) antagonist was bath applied and affected the whole brain. Epileptic activity in telencephalic and other brain structures providing excitatory input to OB INs might also contribute to rhythmic synchronization of the OB network. Ephaptic effects might even elicit synchronous antidromic action potentials in MC axons.

Taken together, the results indicate that GABA(A) mediated inhibition from INs is crucial for the regulation of neuronal excitability in the OB network.

AMPA receptor-dependent control of interneuron activity and mitral cell inhibition

In mammalian brain slices in the absence of background activity, NMDA receptors are critically involved in the activation of granule cells and in the recurrent inhibition of MCs by asynchronous GABA release from IN dendrites (Isaacson and Strowbridge, 1998; Schoppa et al., 1998; Isaacson, 2001). When synaptic background activity is introduced into an OB slice, however, activation of granule cell firing becomes NMDA receptor independent and asynchronous GABA release appears to be strongly diminished (Schoppa, 2006b). Under these conditions, recurrent inhibition is likely to be weak (Schoppa, 2006b). It is therefore unclear how IN firing and inhibition of MCs is controlled during an odor response in the intact OB. I found that the mean odor-evoked somatic Ca^{2+}-signal in INs was reduced by the blockade of AMPA receptors, but not by the blockade of NMDA receptors. Somatic Ca^{2+}-signals in zebrafish MCs and INs reflect action potential firing (Yaksi and Friedrich, 2006; Yaksi et al., 2007). The data therefore indicate that IN firing is controlled primarily by AMPA receptors during an odor response. Nevertheless, individual IN responses were often changed by AP5. Hence, NMDA receptors appear to influence odor responses in a subset of neurons and thereby cause complex effects on spatio-temporal activity patterns within the network.

Although NMDA receptors appear to play a minor role in initiating action potential firing of INs, they may contribute to recurrent inhibition of MCs by triggering asynchronous GABA release from IN dendrites in an action potential-independent fashion (Isaacson and Strowbridge, 1998; Schoppa et al., 1998). If so, however, the blockade of NMDA receptors should increase the ratio between the mean activity of MCs and INs, which was not observed.

The data therefore suggest that the effect of recurrent inhibition by NMDA receptor-dependent asynchronous GABA release at reciprocal synapses on MC firing is, on average, weak compared to the effect of other synaptic pathways.

Unlike inhibition of NMDA receptors, the blockade of AMPA receptors increased the mean response of MCs and decreased the mean somatic Ca^{2+} response of INs. The most likely explanation for these effects is that inhibitory input to MCs during an odor response is mediated primarily by AMPA receptor-dependent action potential firing of INs, consistent with predictions based on data from mammalian brain slices in the presence of synaptic background activity (Schoppa, 2006b). Action potentials invade large portions of the dendritic tree in INs (Egger et al., 2005; Murphy et al., 2005; Zelles et al., 2006) and are thought to trigger GABA release onto multiple postsynaptic MCs. Hence, lateral inhibition, rather than recurrent inhibition, may be the dominant mode of MC inhibition during an odor response. Further experiments are, however, required to test this hypothesis and to identify the synaptic pathways underlying the AMPA receptor-dependent activation of IN firing during an odor response.

GABA(A) and AMPA receptors are required for odor-evoked rhythmical synchronization

The oscillatory synchronization of neuronal ensembles in the OB during an odor response is thought to be based on the reciprocal coupling of MCs and INs by fast excitatory and inhibitory transmission (Rall et al., 1966; Eeckman and Freeman, 1990; Friedman and Strowbridge, 2003). Experiments in mammalian brain slices indicated that the fast inhibitory connection is mediated by GABA(A) receptors (Lagier et al., 2004; Schoppa, 2006a; Lagier et al., 2007) and that the fast excitatory connection is mediated by AMPA receptors (Schoppa, 2006b). Also computational modeling (Bazhenov et al., 2001b), and experiments in the insect antennal lobe (MacLeod and Laurent, 1996; Stopfer et al., 1997) indicate that fast, GABA(A) receptor-mediated inhibition is essential for the oscillatory synchronization of odor-specific subsets of MCs during a response. However, to my knowledge, this has not been tested directly in the intact OB. In agreement to the hypothesis I found oscillatory LFP activity during odor stimulation abolished by the blockade of AMPA receptors and GABA(A) receptors. The NMDA receptor antagonist only reduced oscillation amplitude but did not completely block them. This shows that fast transmitter receptors are required for the

rhythmic synchronization of neuronal ensembles in the OB while the slower NMDA receptors appear not directly involved. Other mechanisms suggested generating LFP oscillations, as voltage-dependent Na^+-channels intrinsic to MC membranes (Desmaisons et al., 1999), oscillatory activity in olfactory sensory neurons (Nikonov et al., 2002) and electrical coupling (Friedman and Strowbridge, 2003) might support network oscillations but are not sufficient by themselves.

Because of their slow kinetics, NMDA receptors are unlikely to be directly involved in fast oscillatory synchronization in the OB. Nevertheless, NMDA receptor antagonists reduced odor-evoked LFP oscillations and slightly increased the oscillation frequency. One possible explanation is that NMDA receptor-mediated depolarization facilitates spiking of INs, which could enhance synchronization. However, NMDA receptor antagonists did not, on average, reduce odor-evoked Ca^{2+}-signals in IN somata. Further experiments are therefore necessary to clarify the role of NMDA receptors in oscillatory synchronization.

Slow temporal modulations of MC response patterns

The slow temporal modulation of MC firing frequencies during an odor response reflects a dynamic reorganization of the firing pattern across the MC population. On a timescale of a few hundred milliseconds the redundancies of activity patterns evoked by chemically related stimuli are reduced (Friedrich and Laurent, 2001; Friedrich et al., 2004; Friedrich and Laurent, 2004). Because GABA(B) receptors influence both the early and the late phase of MC responses, they may be involved in the time-dependent decorrelation of odor-evoked firing patterns across MCs. Although the effect of GABA(B) antagonist on individual responses appears relatively small, this does not rule out the possibility that GABA(B) receptors shape odor-encoding patterns of activity across the population of MCs in important ways. Response amplitudes during late phases of the response are lower on average so that apparently small changes in the firing rates of individual neurons could cause important changes in population firing. Late patterns are decorrelated and therefore contain information about precise odor identity. It is therefore possible that GABA(B) receptors are involved in pattern decorrelation as suggested by computer models (Bazhenov et al., 2001a). Nevertheless, it appears unlikely that pattern decorrelation is mediated exclusively by GABA(B) receptor-dependent mechanisms because responses of projection neurons in insects (Wilson and Laurent, 2005) and responses of MCs in vertebrates are still temporally patterned

in the presence of GABA(B) receptor antagonists. Further studies are therefore required to investigate the role of GABA(B) receptor -mediated inhibition in pattern decorrelation.

Both iGlu receptor antagonists had complex effects on the temporal profile of MC odor responses including changes in the sign. Particularly AP5, further, changed the spatial patterns of activity across MC and IN populations. This is expected, as both receptors drive IN excitation and therefore also affect timing and amount of GABA release. Beyond the level of sensory input asynchronous transmitter release was suggested to cause long-lasting inhibitory influence from granule cells (Wellis and Kauer, 1993; Schoppa et al., 1998). Although the data presented here indicate a dominance of lateral inhibition during odor processing, it does not exclude that such a mechanism enables long-lasting GABA(A) mediated inhibition and thereby is involved in the slow temporal patterning. Recent results indicate that pattern decorrelation is caused, at least in part, by the local sparsening of MC activity patterns in regions where glomerular input is dense and overlapping (Yaksi et al., 2007). The most likely mechanism underlying this local sparsening is the spatially restricted inhibitory feedback from INs.

In addition, iGlu receptor antagonists may modulate other sub-circuits in the OB or the feedback from higher brain regions onto INs which might participate in spatio-temporal modulations.

Functional implications and outlook

IGlu receptors and GABA receptors underlie the basic synaptic transmission in the OB network and therefore provide the basis for odor processing. Under natural conditions, the number and intensity of activated glomeruli varies greatly between different odors and concentrations. The regulation of transmitter release from OSNs through GABA(B) receptors and feedback circuits involving AMPA and GABA(A) receptors may therefore contribute to the robustness of odor representations against changes in stimulus intensity.

Mechanisms modulating the temporal profile of MC odor responses, as GABA(B) receptor mediated presynaptic inhibition and inhibitory feedback from interneurons, likely contribute to decorrelation (Friedrich and Laurent, 2001) that may promote odor discrimination (Rinberg et al., 2006) and prepare odor representations for memory formation (Hasselmo et al., 1990).

The oscillatory synchronization of odor-specific neuronal ensembles has been implicated in odor discrimination in insects (Stopfer et al., 1997) and affords the simultaneous

transmission of different information from the OB to higher brain regions in zebrafish (Friedrich et al., 2004). The synchronization of neuronal ensembles by the help of fast GABA(A) and AMPA receptors therefore contributes to the temporal formatting of odor representations.

I conclude that different receptor types play distinguishable roles for odor processing. The fast GABA(A) and AMPA receptors showed a major impact on firing frequencies during a transient phase immediately after the odor onset. They appear involved and most effective for the adaptation to changing stimulus conditions. The slow GABA(B) and NMDA receptor had no particular influence on the initial phase of the odor response which suggests a different role during odor evoked activity. The interplay of different receptor types apparently allows the parallel performance of different computations. One example is the GABA(A) receptor, that shows that a receptor with fast kinetic might simultaneously be involved in fast and slow synaptic effects. While its interactions with the fast AMPA receptor provide a mechanism for fast neuronal synchronization, its interactions with the slow NMDA receptor might support slow temporal effects through asynchronous transmitter release.

Here I did a first step in the pharmacological analysis of OB network function during odor processing in the intact brain. Pharmacological substances, even though they were receptor specific, induced multiple effects. Further, the effects were unfortunately not localizable to a specific synapse. In future experiments this might be possible by the usage of drugs which are specific for the subunit composition of receptors and /or novel genetic and molecular tools able to target specific cell types (e. g., Zhang et al., 2007).

Acknowledgements

I thank Dr. Rainer Friedrich for giving me the opportunity to perform this scientific project under his supervision and for his scientific and financial support.

I thank Prof. Winfried Denk and Prof. Stephan Frings for the evaluation of my doctoral thesis.

I'm very grateful to all members of the lab for the good time and fruitful discussions. The warm and personal atmosphere in the team made working always a pleasure.

I thank Dr. Julia Bucher and Dr. Andreas Schaefer for their comments on the manuscript.

For the continuous moral support I need to thank particularly my family and Manuela Zehler. Moreover, I thank all my friends and those who personally supported my scientific work although not mentioned here by name.

This study was performed in Department of Biomedical Optics in the Max Planck Institute for Medical Research in Heidelberg.

References

Adrian ED (1942) Olfactory reactions in the brain of the hedgehog. J Physiol 100:459-473.

Alioto TS, Ngai J (2005) The odorant receptor repertoire of teleost fish. BMC Genomics 6:173.

Allison AC (1953) The morphology of the olfactory system in the vertebrates. Biol Rev 28:195-244.

Andres KH (1970) Anatomy and ultrastructure of the olfactory bulb in fish, amphibia, reptiles, birds and mammals. In: Ciba foundation symposium on taste and smell in vertebrates (Wolstenholme GEW, Knight J, eds), pp 177-196. London: Churchill Press.

Aroniadou-Anderjaska V, Ennis M, Shipley MT (1999a) Dendrodendritic recurrent excitation in mitral cells of the rat olfactory bulb. J Neurophysiol 82:489-494.

Aroniadou-Anderjaska V, Ennis M, Shipley MT (1999b) Current-source density analysis in the rat olfactory bulb: laminar distribution of kainate/AMPA- and NMDA-receptor-mediated currents. J Neurophysiol 81:15-28.

Aroniadou-Anderjaska V, Zhou FM, Priest CA, Ennis M, Shipley MT (2000) Tonic and synaptically evoked presynaptic inhibition of sensory input to the rat olfactory bulb via GABA(B) heteroreceptors. J Neurophysiol 84:1194-1203.

Aungst JL, Heyward PM, Puche AC, Karnup SV, Hayar A, Szabo G, Shipley MT (2003) Centre-surround inhibition among olfactory bulb glomeruli. Nature 426:623-629.

Azouz R, Jensen MS, Yaari Y (1996) Ionic basis of spike after-depolarization and burst generation in adult rat hippocampal CA1 pyramidal cells. J Physiol 492 (Pt 1):211-223.

Barnard EA, Skolnick P, Olsen RW, Mohler H, Sieghart W, Biggio G, Braestrup C, Bateson AN, Langer SZ (1998) International Union of Pharmacology. XV. Subtypes of gamma-aminobutyric acidA receptors: classification on the basis of subunit structure and receptor function. Pharmacol Rev 50:291-313.

Bazhenov M, Stopfer M, Rabinovich M, Abarbanel HDI, Sejnowski TJ, Laurent G (2001a) Model of cellular and network mechanisms for odor-evoked temporal patterning in the locust antennal lobe. Neuron 30:569-581.

Bazhenov M, Stopfer M, Rabinovich M, Huerta R, Abarbanel HDI, Sejnowski TJ, Laurent G (2001b) Model of transient oscillatory synchronization in the locust antennal lobe. Neuron 30:553-567.

Belluscio L, Katz LC (2001) Symmetry, stereotypy, and topography of odorant representations in mouse olfactory bulbs. J Neurosci 21:2113-2122.

Berkowicz DA, Trombley PQ, Shepherd GM (1994) Evidence for glutamate as the olfactory receptor cell neurotransmitter. J Neurophysiol 71:2557-2561.

Bonino M, Cantino D, Sassoe-Pognetto M (1999) Cellular and subcellular localization of gamma-aminobutyric acidB receptors in the rat olfactory bulb. Neurosci Lett 274:195-198.

Bormann J (2000) The 'ABC' of GABA receptors. Trends Pharmacol Sci 21:16-19.

Bowery NG, Hudson AL, Price GW (1987) GABAA and GABAB receptor site distribution in the rat central nervous system. Neuroscience 20:365-383.

Bressler SL, Freeman WJ (1980) Frequency analysis of olfactory system EEG in cat, rabbit, and rat. Electroencephalogr Clin Neurophysiol 50:19-24.

Broadwell RD, Jacobowitz DM (1976) Olfactory relationships of the telencephalon and diencephalon in the rabbit. III. The ipsilateral centrifugal fibers to the olfactory bulbar and retrobulbar formations. J Comp Neurol 170:321-345.

Buck LB (1996) Information coding in the vertebrate olfactory system. Annu Rev Neurosci 19:517-544.
Buonviso N, Chaput MA (1990) Response similarity to odors in olfactory bulb output cells presumed to be connected to the same glomerulus: electrophysiological study using simultaneous single-unit recordings. J Neurophysiol 63:447-454.
Buonviso N, Chaput MA, Berthommier F (1992) Temporal pattern analyses in pairs of neighboring mitral cells. J Neurophysiol 68:417-424.
Calver AR, Davies CH, Pangalos M (2002) GABA(B) receptors: from monogamy to promiscuity. Neurosignals 11:299-314.
Carlson GC, Shipley MT, Keller A (2000) Long-lasting depolarizations in mitral cells of the rat olfactory bulb. J Neurosci 20:2011-2021.
Carson KA, Burd GD (1980) Localization of acetylcholinesterase in the main and accessory olfactory bulbs of the mouse by light and electron microscopic histochemistry. J Comp Neurol 191:353-371.
Castillo PE, Carleton A, Vincent JD, Lledo PM (1999) Multiple and opposing roles of cholinergic transmission in the main olfactory bulb. J Neurosci 19:9180-9191.
Chen WR, Xiong W, Shepherd GM (2000a) Analysis of relations between NMDA receptors and GABA release at olfactory bulb reciprocal synapses. Neuron 25:625-633.
Chen WR, Xiong W, Shepherd GM (2000b) Analysis of relations between NMDA receptors and GABA release at olfactory bulb reciprocal synapses. Neuron 25:625-633.
Christie JM, Westbrook GL (2006) Lateral excitation within the olfactory bulb. J Neurosci 26:2269-2277.
Christie JM, Bark C, Hormuzdi SG, Helbig I, Monyer H, Westbrook GL (2005) Connexin36 mediates spike synchrony in olfactory bulb glomeruli. Neuron 46:761-772.
Chu DC, Albin RL, Young AB, Penney JB (1990) Distribution and kinetics of GABAB binding sites in rat central nervous system: a quantitative autoradiographic study. Neuroscience 34:341-357.
Czesnik D, Nezlin L, Rabba J, Muller B, Schild D (2001) Noradrenergic modulation of calcium currents and synaptic transmission in the olfactory bulb of Xenopus laevis tadpoles. Eur J Neurosci 13:1093-1100.
Derkach VA, Oh MC, Guire ES, Soderling TR (2007) Regulatory mechanisms of AMPA receptors in synaptic plasticity. Nat Rev Neurosci 8:101-113.
Desmaisons D, Vincent J-D, Lledo P-M (1999) Control of action potential timing by intrinsic subthreshold oscillations in olfactory bulb output neurons. J Neurosci 19:10727-10737.
Didier A, Carleton A, Bjaalie JG, Vincent JD, Ottersen OP, Storm-Mathisen J, Lledo PM (2001) A dendrodendritic reciprocal synapse provides a recurrent excitatory connection in the olfactory bulb. Proc Natl Acad Sci U S A 98:6441-6446.
Dingledine R, Borges K, Bowie D, Traynelis SF (1999) The glutamate receptor ion channels. Pharmacol Rev 51:7-61.
Duchamp-Viret P, Chaput MA, Duchamp A (1999) Odor response properties of rat olfactory receptor neurons. Science 284:2171-2174.
Duchamp-Viret P, Delaleu JC, Duchamp A (2000) GABA(B)-mediated action in the frog olfactory bulb makes odor responses more salient. Neuroscience 97:771-777.
Dulac C (1997) How does the brain smell? Neuron 19:477-480.
Edwards JG, Michel WC (2002) Odor-stimulated glutamatergic neurotransmission in the zebrafish olfactory bulb. J Comp Neurol 454:294-309.
Eeckman FH, Freeman WJ (1990) Correlations between unit firing and EEG in the rat olfactory system. Brain Res 528:238-244.

Egger V, Svoboda K, Mainen ZF (2005) Dendrodendritic synaptic signals in olfactory bulb granule cells: local spine boost and global low-threshold spike. J Neurosci 25:3521-3530.

Ennis M, Zimmer LA, Shipley MT (1996) Olfactory nerve stimulation activates rat mitral cells via NMDA and non-NMDA receptors in vitro. Neuroreport 7:989-992.

Fallon JH, Moore RY (1978) Catecholamine innervation of the basal forebrain. III. Olfactory bulb, anterior olfactory nuclei, olfactory tubercle and piriform cortex. J Comp Neurol 180:533-544.

Friedman D, Strowbridge BW (2000) Functional role of NMDA autoreceptors in olfactory mitral cells. J Neurophysiol 84:39-50.

Friedman D, Strowbridge BW (2003) Both electrical and chemical synapses mediate fast network oscillations in the olfactory bulb. J Neurophysiol 89:2601-2610.

Friedrich RW, Korsching SI (1997) Combinatorial and chemotopic odorant coding in the zebrafish olfactory bulb visualized by optical imaging. Neuron 18:737-752.

Friedrich RW, Korsching SI (1998) Chemotopic, combinatorial and noncombinatorial odorant representations in the olfactory bulb revealed using a voltage-sensitive axon tracer. J Neurosci 18:9977-9988.

Friedrich RW, Laurent G (2001) Dynamic optimization of odor representations in the olfactory bulb by slow temporal patterning of mitral cell activity. Science 291:889-894.

Friedrich RW, Laurent G (2004) Dynamics of olfactory bulb input and output activity during odor stimulation in zebrafish. J Neurophysiol 91:2658-2669.

Friedrich RW, Habermann CJ, Laurent G (2004) Multiplexing using synchrony in the zebrafish olfactory bulb. Nature Neurosci 7:862-871.

Fuller CL, Yettaw HK, Byrd CA (2006) Mitral cells in the olfactory bulb of adult zebrafish (Danio rerio): morphology and distribution. J Comp Neurol, in press.

Gelperin A, Tank DW (1990) Odour-modulated collective network oscillations of olfactory interneurons in a terrestrial mollusc. Nature 345:437-440.

Goldman AL, Van der Goes van Naters W, Lessing D, Warr CG, Carlson JR (2005) Coexpression of two functional odor receptors in one neuron. Neuron 45:661-666.

Gomez C, Brinon JG, Colado MI, Orio L, Vidal M, Barbado MV, Alonso JR (2006) Differential effects of unilateral olfactory deprivation on noradrenergic and cholinergic systems in the main olfactory bulb of the rat. Neuroscience 141:2117-2128.

Gray CM, Skinner JE (1988) Field potential response changes in the rabbit olfactory bulb accompany behavioral habituation during the repeated presentation of unreinforced odors. Exp Brain Res 73:189-197.

Halabisky B, Friedman D, Radojicic M, Strowbridge BW (2000) Calcium influx through NMDA receptors directly evokes GABA release in olfactory bulb granule cells. J Neurosci 20:5124-5134.

Hamann M, Desarmenien M, Desaulles E, Bader MF, Feltz P (1988) Quantitative evaluation of the properties of a pyridazinyl GABA derivative (SR 95531) as a GABAA competitive antagonist. An electrophysiological approach. Brain Res 442:287-296.

Hamilton KA, Kauer JS (1989) Patterns of intracellular potentials in salamander mitral/tufted cells in response to odor stimulation. J Neurophysiol 62:609-625.

Hardy A, Palouzier-Paulignan B, Duchamp A, Royet JP, Duchamp-Viret P (2005) 5-Hydroxytryptamine action in the rat olfactory bulb: in vitro electrophysiological patch-clamp recordings of juxtaglomerular and mitral cells. Neuroscience 131:717-731.

Hasselmo ME, Wilson MA, Anderson BP, Bower JM (1990) Associative memory function in piriform (olfactory) cortex: computational modeling and neuropharmacology. Cold Spring Harb Symp Quant Biol 55:599-610.

Hayar A, Karnup S, Shipley MT, Ennis M (2004) Olfactory bulb glomeruli: external tufted cells intrinsically burst at theta frequency and are entrained by patterned olfactory input. J Neurosci 24:1190-1199.

Hayar A, Heyward PM, Heinbockel T, Shipley MT, Ennis M (2001) Direct excitation of mitral cells via activation of alpha1-noradrenergic receptors in rat olfactory bulb slices. J Neurophysiol 86:2173-2182.

Hefft S, Jonas P (2005) Asynchronous GABA release generates long-lasting inhibition at a hippocampal interneuron-principal neuron synapse. Nat Neurosci 8:1319-1328.

Higashijima S, Masino MA, Mandel G, Fetcho JR (2003) Imaging neuronal activity during zebrafish behavior with a genetically encoded calcium indicator. J Neurophysiol 90:3986-3997.

Hsia AY, Vincent JD, Lledo PM (1999) Dopamine depresses synaptic inputs into the olfactory bulb. J Neurophysiol 82:1082-1085.

Ichikawa T, Hirata Y (1986) Organization of choline acetyltransferase-containing structures in the forebrain of the rat. J Neurosci 6:281-292.

Imboden M, Devignot V, Korn H, Goblet C (2001) Regional distribution of glycine receptor messenger RNA in the central nervous system of zebrafish. Neuroscience 103:811-830.

Isaac JT, Ashby M, McBain CJ (2007) The role of the GluR2 subunit in AMPA receptor function and synaptic plasticity. Neuron 54:859-871.

Isaacson JS (1999a) Glutamate spillover mediates excitatory transmission in the rat olfactory bulb. Neuron 23:377-384.

Isaacson JS (1999b) Glutamate spillover mediates excitatory transmission in the rat olfactory bulb. Neuron 23:377-384.

Isaacson JS (2000) Spillover in the spotlight. Curr Biol 10:R475-477.

Isaacson JS (2001) Mechanisms governing dendritic gamma-aminobutyric acid (GABA) release in the rat olfactory bulb. Proc Natl Acad Sci U S A 98:337-342.

Isaacson JS, Strowbridge BW (1998) Olfactory reciprocal synapses: dendritic signaling in the CNS. Neuron 20:749-761.

Isaacson JS, Vitten H (2003) GABA(B) receptors inhibit dendrodendritic transmission in the rat olfactory bulb. J Neurosci 23:2032-2039.

Jahr CE, Nicoll RA (1982) An intracellular analysis of dendrodendritic inhibition in the turtle in vitro olfactory bulb. J Physiol Lond 326:213-234.

Jonas P (2000) The Time Course of Signaling at Central Glutamatergic Synapses. News Physiol Sci 15:83-89.

Kashiwadani H, Sasaki YF, Uchida N, Mori K (1999) Synchronized oscillatory discharges of mitral/tufted cells with different molecular receptive ranges in the rabbit olfactory bulb. J Neurophysiol 82:1786-1792.

Kay LM, Laurent G (1999) Odor- and context-dependent modulation of mitral cell activity in behaving rats. Nat Neurosci 2:1003-1009.

Kiselycznyk CL, Zhang S, Linster C (2006) Role of centrifugal projections to the olfactory bulb in olfactory processing. Learn Mem 13:575-579.

Knaus HG, Schwarzer C, Koch RO, Eberhart A, Kaczorowski GJ, Glossmann H, Wunder F, Pongs O, Garcia ML, Sperk G (1996) Distribution of high-conductance Ca(2+)-activated K+ channels in rat brain: targeting to axons and nerve terminals. J Neurosci 16:955-963.

Kornau HC (2006) GABA(B) receptors and synaptic modulation. Cell Tissue Res 326:517-533.

Kratskin I, Kenigfest N, Rio JP, Djediat C, Reperant J (2006) Immunocytochemical localization of the GABA(B2) receptor subunit in the glomeruli of the mouse main olfactory bulb. Neurosci Lett 402:121-125.
Laaris N, Puche A, Ennis M (2007) Complementary postsynaptic activity patterns elicited in olfactory bulb by stimulation of mitral/tufted and centrifugal fiber inputs to granule cells. J Neurophysiol 97:296-306.
Lagier S, Carleton A, Lledo PM (2004) Interplay between local GABAergic interneurons and relay neurons generates gamma oscillations in the rat olfactory bulb. J Neurosci 24:4382-4392.
Lagier S, Panzanelli P, Russo RE, Nissant A, Bathellier B, Sassoe-Pognetto M, Fritschy JM, Lledo PM (2007) GABAergic inhibition at dendrodendritic synapses tunes gamma oscillations in the olfactory bulb. Proc Natl Acad Sci U S A 104:7259-7264.
Lam YW, Cohen LB, Wachowiak M, Zochowski MR (2000) Odors elicit three different oscillations in the turtle olfactory bulb. J Neurosci 20:749-762.
Laurent G (2002) Olfactory network dynamics and the coding of multidimensional signals. Nat Rev Neurosci 3:884-895.
Laurent G, Davidowitz H (1994) Encoding of olfactory information with oscillating neural assemblies. Science 265:1872-1875.
Leveteau J, MacLeod P (1966) Olfactory discrimination in the rabbit olfactory glomerulus. Science 153:175-176.
Li J, Mack JA, Souren M, Yaksi E, Higashijima S, Mione M, Fetcho JR, Friedrich RW (2005) Early development of functional spatial maps in the zebrafish olfactory bulb. J Neurosci 25:5784-5795.
Liu SJ, Zukin RS (2007) Ca2+-permeable AMPA receptors in synaptic plasticity and neuronal death. Trends Neurosci 30:126-134.
Lowe G (2002) Inhibition of backpropagating action potentials in mitral cell secondary dendrites. J Neurophysiol 88:64-85.
Luo M, Katz LC (2001) Response correlation maps of neurons in the Mammalian olfactory bulb. Neuron 32:1165-1179.
Luskin MB, Price JL (1983) The topographic organization of associational fibers of the olfactory system in the rat, including centrifugal fibers to the olfactory bulb. J Comp Neurol 216:264-291.
MacLeod K, Laurent G (1996) Distinct mechanisms for synchronization and temporal patterning of odor-encoding neural assemblies. Science 274:976-979.
MacLeod NK (1976) Spontaneous activity of single neurons in the olfactory bulb of the rainbow trout (Salmo gairdneri) and iots modulation by olfactory stimyulation with amino acids. Exp Brain Res 25:267-278.
Macrides F, Davis BJ, Youngs WM, Nadi NS, Margolis FL (1981) Cholinergic and catecholaminergic afferents to the olfactory bulb in the hamster: a neuroanatomical, biochemical, and histochemical investigation. J Comp Neurol 203:495-514.
Malnic B, Hirono J, Sato T, Buck LB (1999) Combinatorial receptor codes for odors. Cell 96:713-723.
Margeta-Mitrovic M, Mitrovic I, Riley RC, Jan LY, Basbaum AI (1999) Immunohistochemical localization of GABA(B) receptors in the rat central nervous system. J Comp Neurol 405:299-321.
Martin C, Gervais R, Messaoudi B, Ravel N (2006) Learning-induced oscillatory activities correlated to odour recognition: a network activity. Eur J Neurosci 23:1801-1810.
Mathieson WB, Maler L (1988) Morphological and electrophysiological properties of a novel in vitro preparation: the electrosenspry lateral line lobe brain slice. J Comp Physiol A 163:489-506.

McCormick DA, Contreras D (2001) On the cellular and network bases of epileptic seizures. Annu Rev Physiol 63:815-846.
McGann JP, Pirez N, Gainey MA, Muratore C, Elias AS, Wachowiak M (2005) Odorant representations are modulated by intra- but not interglomerular presynaptic inhibition of olfactory sensory neurons. Neuron 48:1039-1053.
McLean JH, Shipley MT (1987) Serotonergic afferents to the rat olfactory bulb: I. Origins and laminar specificity of serotonergic inputs in the adult rat. J Neurosci 7:3016-3028.
McLean JH, Darby-King A, Hodge E (1996) 5-HT2 receptor involvement in conditioned olfactory learning in the neonate rat pup. Behav Neurosci 110:1426-1434.
Meredith M (1986) Patterned response to odor in mammalian olfactory bulb: the influence of intensity. J Neurophysiol 56:572-597.
Mesulam MM, Mufson EJ, Wainer BH, Levey AI (1983) Central cholinergic pathways in the rat: an overview based on an alternative nomenclature (Ch1-Ch6). Neuroscience 10:1185-1201.
Michels G, Moss SJ (2007) GABAA receptors: properties and trafficking. Crit Rev Biochem Mol Biol 42:3-14.
Miyamoto E (2006) Molecular mechanism of neuronal plasticity: induction and maintenance of long-term potentiation in the hippocampus. J Pharmacol Sci 100:433-442.
Mombaerts P, Wang F, Dulac C, Chao SK, Nemes A, Mendelsohn M, Edmondson J, Axel R (1996) Visualizing an olfactory sensory map. Cell 87:675-686.
Mori K, Nagao H, Yoshihara Y (1999) The olfactory bulb: coding and processing of odor molecule information. Science 286:711-715.
Mori K, Takahashi YK, Igarashi KM, Yamaguchi M (2006) Maps of odorant molecular features in the mammalian olfactory bulb. Physiol Rev 86:409-433.
Moriizumi T, Tsukatani T, Sakashita H, Miwa T (1994) Olfactory disturbance induced by deafferentation of serotonergic fibers in the olfactory bulb. Neuroscience 61:733-738.
Murphy GJ, Darcy DP, Isaacson JS (2005) Intraglomerular inhibition: signaling mechanisms of an olfactory microcircuit. Nat Neurosci 8:354-364.
Nickell WT, Behbehani MM, Shipley MT (1994) Evidence for GABAB-mediated inhibition of transmission from the olfactory nerve to mitral cells in the rat olfactory bulb. Brain Res Bull 35:119-123.
Nikonov AA, Parker JM, Caprio J (2002) Odorant-induced olfactory receptor neural oscillations and their modulation of olfactory bulbar responses in the channel catfish. J Neurosci 22:2352-2362.
Nowycky MC, Mori K, Shepherd GM (1981) Blockade of synaptic inhibition reveals long-lasting synaptic excitation in isolated turtle olfactory bulb. J Neurophysiol 46:649-658.
Nutt D (2006) GABAA receptors: subtypes, regional distribution, and function. J Clin Sleep Med 2:S7-11.
Palouzier-Paulignan B, Duchamp-Viret P, Hardy AB, Duchamp A (2002) GABA(B) receptor-mediated inhibition of mitral/tufted cell activity in the rat olfactory bulb: a whole-cell patch-clamp study in vitro. Neuroscience 111:241-250.
Panzanelli P, Lopez-Bendito G, Lujan R, Sassoe-Pognetto M (2004) Localization and developmental expression of GABA(B) receptors in the rat olfactory bulb. J Neurocytol 33:87-99.
Pinching AJ, Powell TP (1972) The termination of centrifugal fibres in the glomerular layer of the olfactory bulb. J Cell Sci 10:621-635.
Pressler RT, Strowbridge BW (2006) Blanes Cells Mediate Persistent Feedforward Inhibition onto Granule Cells in the Olfactory Bulb. Neuron 49:889-904.
Pressler RT, Inoue T, Strowbridge BW (2007) Muscarinic receptor activation modulates granule cell excitability and potentiates inhibition onto mitral cells in the rat olfactory bulb. J Neurosci 27:10969-10981.

Puopolo M, Belluzzi O (2001) NMDA-dependent, network-driven oscillatory activity induced by bicuculline or removal of Mg2+ in rat olfactory bulb neurons. Eur J Neurosci 13:92-102.
Rall W, Shepherd GM, Reese TS, Brightman MW (1966) Dendrodendritic synaptic pathway for inhibition in the olfactory bulb. Exp Neurol 14:44-56.
Ressler KJ, Sullivan SL, Buck LB (1994) Information coding in the olfactory system: evidence for a stereotyped and highly organized epitope map in the olfactory bulb. Cell 79:1245-1255.
Rinberg D, Koulakov A, Gelperin A (2006) Speed-accuracy tradeoff in olfaction. Neuron 51:351-358.
Rosenmund C, Stern-Bach Y, Stevens CF (1998) The tetrameric structure of a glutamate receptor channel. Science 280:1596-1599.
Sakaba T, Neher E (2003) Direct modulation of synaptic vesicle priming by GABA(B) receptor activation at a glutamatergic synapse. Nature 424:775-778.
Salin PA, Lledo PM, Vincent JD, Charpak S (2001) Dendritic glutamate autoreceptors modulate signal processing in rat mitral cells. J Neurophysiol 85:1275-1282.
Sassoe-Pognetto M, Ottersen OP (2000) Organization of ionotropic glutamate receptors at dendrodendritic synapses in the rat olfactory bulb. J Neurosci 20:2192-2201.
Satou M (1990) Synaptic organization, local neuronal circuitry, and functional segregation of the teleost olfactory bulb. Prog Neurobiol 34:115-142.
Satou M, Hoshikawa R, Sato Y, Okawa K (2006) An in vitro study of long-term potentiation in the carp (Cyprinus carpio L.) olfactory bulb. J Comp Physiol A Neuroethol Sens Neural Behav Physiol 192:135-150.
Schoppa NE (2006a) Synchronization of olfactory bulb mitral cells by precisely timed inhibitory inputs. Neuron 49:271-283.
Schoppa NE (2006b) AMPA/kainate receptors drive rapid output and precise synchrony in olfactory bulb granule cells. J Neurosci 26:12996-13006.
Schoppa NE, Westbrook GL (2002) AMPA autoreceptors drive correlated spiking in olfactory bulb glomeruli. Nat Neurosci 5:1194-1202.
Schoppa NE, Kinzie JM, Sahara Y, Segerson TP, Westbrook GL (1998) Dendrodendritic inhibition in the olfactory bulb is driven by NMDA receptors. J Neurosci 18:6790-6802.
Sheardown MJ, Nielsen EO, Hansen AJ, Jacobsen P, Honore T (1990) 2,3-Dihydroxy-6-nitro-7-sulfamoyl-benzo(F)quinoxaline: a neuroprotectant for cerebral ischemia. Science 247:571-574.
Shepherd GM (1994) Discrimination of molecular signals by the olfactory receptor neuron. Neuron 13:771-790.
Shepherd GM, Chen WR, Greer CA (2004) Olfactory bulb. In: The synaptic organization of the brain (Shepherd GM, ed), pp 165-216. Oxford: Oxford University Press.
Shepherd JD, Huganir RL (2007) The cell biology of synaptic plasticity: AMPA receptor trafficking. Annu Rev Cell Dev Biol 23:613-643.
Shipley MT, Halloran FJ, de la Torre J (1985) Surprisingly rich projection from locus coeruleus to the olfactory bulb in the rat. Brain Res 329:294-299.
Sicard G, Holley A (1984) Receptor cell responses to odorants: similarities and differences among odorants. Brain Res 292:283-296.
Sivilotti L, Nistri A (1991) GABA receptor mechanisms in the central nervous system. Prog Neurobiol 36:35-92.
Smith TC, Jahr CE (2002) Self-inhibition of olfactory bulb neurons. Nat Neurosci 1:1.
Spors H, Wachowiak M, Cohen LB, Friedrich RW (2006) Temporal dynamics and latency patterns of receptor neuron input to the olfactory bulb. J Neurosci 26:1247-1259.

Stewart WB, Kauer JS, Shepherd GM (1979) Functional organization of rat olfactory bulb analysed by the 2-deoxyglucose method. J Comp Neurol 185:715-734.
Stopfer M, Bhagavan S, Smith BH, Laurent G (1997) Impaired odour discrimination on desynchronization of odour-encoding neural assemblies. Nature 390:70-74.
Tabor R, Friedrich RW (2008) Pharmacological analysis of ionotropic glutamate receptor function in neuronal circuits of the zebrafish olfactory bulb. PLoS ONE 3:e1416.
Tabor R, Yaksi E, Weislogel JM, Friedrich RW (2004) Processing of odor mixtures in the zebrafish olfactory bulb. J Neurosci 24:6611-6620.
Tani A, Yoshihara Y, Mori K (1992) Increase in cytoplasmic free Ca2+ elicited by noradrenalin and serotonin in cultured local interneurons of mouse olfactory bulb. Neuroscience 49:193-199.
Tichelaar W, Safferling M, Keinanen K, Stark H, Madden DR (2004) The Three-dimensional Structure of an Ionotropic Glutamate Receptor Reveals a Dimer-of-dimers Assembly. J Mol Biol 344:435-442.
Traub RD, Borck C, Colling SB, Jefferys JG (1996) On the structure of ictal events in vitro. Epilepsia 37:879-891.
Trombley PQ, Westbrook GL (1990) Excitatory synaptic transmission in cultures of rat olfactory bulb. J Neurophysiol 64:598-606.
Trombley PQ, Shepherd GM (1994) Glycine exerts potent inhibitory actions on mammalian olfactory bulb neurons. J Neurophysiol 71:761-767.
Trombley PQ, Hill BJ, Horning MS (1999) Interactions between GABA and glycine at inhibitory amino acid receptors on rat olfactory bulb neurons. J Neurophysiol 82:3417-3422.
Uchida N, Takahashi YK, Tanifuji M, Mori K (2000) Odor maps in the mammalian olfactory bulb: domain organization and odorant structural features. Nat Neurosci 3:1035-1043.
Ueno S, Bracamontes J, Zorumski C, Weiss DS, Steinbach JH (1997) Bicuculline and gabazine are allosteric inhibitors of channel opening of the GABAA receptor. J Neurosci 17:625-634.
Urban NN, Sakmann B (2002) Reciprocal intraglomerular excitation and intra- and interglomerular lateral inhibition between mouse olfactory bulb mitral cells. J Physiol 542:355-367.
Vassar R, Ngai J, Axel R (1993) Spatial segregation of odorant receptor expression in the mammalian olfactory epithelium. Cell 74:309-318.
Vassar R, Chao SK, Sitcheran R, Nunez JM, Vosshall LB, Axel R (1994) Topographic organization of sensory projections to the olfactory bulb. Cell 79:981-991.
Vucinic D, Cohen LB, Kosmidis EK (2006) Interglomerular center-surround inhibition shapes odorant-evoked input to the mouse olfactory bulb in vivo. J Neurophysiol 95:1881-1887.
Wachowiak M, Cohen LB (1999a) Presynaptic inhibition of primary olfactory afferents mediated by different mechanisms in lobster and turtle. J Neurosci 19:8808-8817.
Wachowiak M, Cohen LB (1999b) Presynaptic inhibition of primary olfactory afferents mediated by different mechanisms in lobster and turtle. J Neurosci 19:8808-8817.
Wachowiak M, Cohen LB (2001) Representation of odorants by receptor neuron input to the mouse olfactory bulb. Neuron 32:723-735.
Wachowiak M, Shipley MT (2006) Coding and synaptic processing of sensory information in the glomerular layer of the olfactory bulb. Semin Cell Dev Biol 17:411-423.
Wachowiak M, Denk W, Friedrich RW (2004) Functional organization of sensory input to the olfactory bulb glomerulus analyzed by two-photon calcium imaging. Proc Natl Acad Sci USA 101:9097-9102.

Wachowiak M, McGann JP, Heyward PM, Shao Z, Puche AC, Shipley MT (2005a) Inhibition of olfactory receptor neuron input to olfactory bulb glomeruli mediated by suppression of presynaptic calcium influx. J Neurophysiol.

Wachowiak M, McGann JP, Heyward PM, Shao Z, Puche AC, Shipley MT (2005b) Inhibition [corrected] of olfactory receptor neuron input to olfactory bulb glomeruli mediated by suppression of presynaptic calcium influx. J Neurophysiol 94:2700-2712.

Wellis DP, Kauer JS (1993) GABAA and glutamate receptor involvement in dendrodendritic synaptic interactions from salamander olfactory bulb. J Physiol 469:315-339.

Wellis DP, Scott JW, Harrison TA (1989) Discrimination among odorants by single neurons of the rat olfactory bulb. J Neurophysiol 61:1161-1177.

Wilson DA, Fletcher ML, Sullivan RM (2004) Acetylcholine and olfactory perceptual learning. Learn Mem 11:28-34.

Wilson RI, Laurent G (2005) Role of GABAergic inhibition in shaping odor-evoked spatiotemporal patterns in the Drosophila antennal lobe. J Neurosci 25:9069-9079.

Yaksi E, Friedrich RW (2006) Reconstruction of firing rate changes across neuronal populations by temporally deconvolved Ca^{2+} imaging. Nat Methods 3:377-383.

Yaksi E, Judkewitz B, Friedrich RW (2007) Topological Reorganization of Odor Representations in the Olfactory Bulb. PLoS Biol 5:e178.

Yokoi M, Mori K, Nakanishi S (1995) Refinement of odor molecule tuning by dendrodendritic synaptic inhibition in the olfactory bulb. Proc Natl Acad Sci USA 92:3371-3375.

Zaborszky L, Carlsen J, Brashear HR, Heimer L (1986) Cholinergic and GABAergic afferents to the olfactory bulb in the rat with special emphasis on the projection neurons in the nucleus of the horizontal limb of the diagonal band. J Comp Neurol 243:488-509.

Zelles T, Boyd JD, Hardy AB, Delaney KR (2006) Branch-specific Ca2+ influx from Na+-dependent dendritic spikes in olfactory granule cells. J Neurosci 26:30-40.

Zhang F, Aravanis AM, Adamantidis A, de Lecea L, Deisseroth K (2007) Circuit-breakers: optical technologies for probing neural signals and systems. Nat Rev Neurosci 8:577-581.

Zhang X, Rodriguez I, Mombaerts P, Firestein S (2004) Odorant and vomeronasal receptor genes in two mouse genome assemblies. Genomics 83:802-811.